FLSs support pseudoemperipolesis [21]. Our results indicate that LPA upregulated the expression of VCAM and ICAM on RA FLSs, which was blocked by the LPA_1 antagonist. Thus, LPA may enhance pseudoemperipolesis via the upregulation of VCAM and ICAM expression on RA FLSs through LPA_1. Interestingly, CXCL12 production by RA FLSs was not altered by LPA simulation. Stimulation of lymphocytes by LPA via LPA_1 may also contribute to the enhanced pseudoemperipolesis. In this regard, it has been reported that LPA induced chemokinesis in T cells [25] and lymphocyte transmigration through high endothelial venules [26,27]. Further studies are needed to clarify the effects of LPA–LPA_1 signaling for the lymphocytes on pseudoemperipolesis.

The hyperplastic rheumatoid pannus is characterized by an overabundance of FLSs [2]. This cellular excess stems largely from an imbalance between the proliferation and apoptosis of FLSs [2]. The migration of RA FLSs may also contribute to pannus formation [2]. Our results show that LPA induced the proliferation and migration of FLSs, which was inhibited by the LPA_1 antagonist. Moreover, in a recent study, researchers reported that LPA suppressed tumor necrosis factor–induced apoptosis on RA FLSs via LPA_1 [28]. Therefore, it is suggested that the LPA–LPA_1 signaling also contributed to the cellular excess and migration of FLSs in the RA synovium.

In this study, we show that there are important roles of LPA–LPA_1 signaling on RA FLS stimulation. However, the effects of LPA signals via LPA_{2-6} remain unclear, although RA FLSs also expressed LPA_{2-6}. Further studies are warranted to elucidate the roles of LPA_{2-6} in LPA stimulation of FLSs by using each of the LPA receptor–specific antagonists or FLSs from each LPA receptor–deficient mouse.

It was shown that conditional genetic ablation of ATX, which generates LPA via hydrolysis of lysophosphatidylcholine, in mesenchymal cells resulted in disease attenuation in animal models of arthritis [12]. We have also found that LPA_1 is essential for the development of arthritis in collagen-induced arthritis [15]. The ATX–LPA–LPA_1 axis may play an important role in the development of arthritis.

Conclusion

Our study suggests that LPA–LPA_1 signaling in FLSs may contribute to the pathogenesis of RA by inducing proliferation, production of inflammatory mediators, pseudoemperipolesis and migration on RA FLSs. Thus, LPA_1 could be a promising therapeutic target for RA.

Abbreviations

ATX: Autotaxin; CCL2: Chemokine (C-C motif) ligand 2; CXCL12: Chemokine (C-X-C motif) ligand 12; DMEM: Dulbecco's modified Eagle's medium; Edg: Endothelial cell differentiation gene; ELISA: Enzyme-linked immunosorbent assay; FCS: Fetal calf serum; FLS: Fibroblast-like synoviocyte; ICAM: Intercellular adhesion molecule; IL: Interleukin; LPA: Lysophosphatidic acid; mAb: Monoclonal antibody; MMP-3: Metalloproteinase 3; OA: Osteoarthritis; RA: Rheumatoid arthritis; SEM: Standard error of the mean; VCAM: Vascular cell adhesion molecule; VEGF: Vascular endothelial growth factor.

Competing interests

The authors declare that they have no competing interests.

Authors' contributions

YM participated in the design of the study, carried out the experiments and statistical analysis and drafted the manuscript. CM and CS assisted in carrying out the experiments and with manuscript preparation. YI assisted in data interpretation and manuscript preparation. WY and KS collected the clinical materials and assisted in data interpretation and manuscript preparation. MH, MM, NM and TN conceived of the study, participated in its design and coordination, and helped to draft the manuscript. All authors read and approved the final manuscript.

Acknowledgements

We thank Prof. Timothy J Wright (Otsuma Women's University, Tokyo, Japan) for his helpful advice and for improving the readability of this manuscript. This work was supported in part by the Japanese Ministry of Education, Global Center of Excellence (GCOE) Program, International Research Center for Molecular Science in Tooth and Bone Diseases, and Takeda Science Foundation.

Author details

[1]Department of Medicine and Rheumatology, Graduate School of Medical and Dental Sciences, Tokyo Medical and Dental University, 1-5-45, Yushima, Bunkyo-ku, Tokyo 113-8519, Japan. [2]Department of Dermatology, Tokyo Medical University, 6-7-1, Nishi-Shinjuku, Shinjuku-ku, Tokyo 160-0023, Japan. [3]Department of Molecular Biology, School of Medicine, University of Occupational and Environmental Health, 1-1 Iseigaoka, Yahatanishi-ku, Kitakyushu, Fukuoka 807-8555, Japan. [4]Department of Clinical Research Medicine, Teikyo University, 2-11-1, Kaga, Itabashi-ku, Tokyo 173-8605, Japan. [5]Sonoda Joint Replacement and Sports Medical Center, 1-21-10, Hogima, Adachi-ku, Tokyo 121-0064, Japan. [6]Department of Pharmacovigilance, Graduate School of Medical and Dental Sciences, Tokyo Medical and Dental University, 1-5-45, Yushima, Bunkyo-ku, Tokyo 113-8519, Japan. [7]Interdisciplinary Program for Biomedical Sciences, Osaka University, 2-2, Yamada-oka, Suita, Osaka 565-0871, Japan.

Received: 11 April 2014 Accepted: 22 September 2014
Published online: 02 October 2014

References

1. Kinne RW, Bräuer R, Stuhlmüller B, Palombo-Kinne E, Burmester GR: **Macrophages in rheumatoid arthritis.** *Arthritis Res* 2000, **2**:189–202.
2. Bottini N, Firestein GS: **Duality of fibroblast-like synoviocytes in RA: passive responders and imprinted aggressors.** *Nat Rev Rheumatol* 2013, **9**:24–33.
3. Aoki J: **Mechanisms of lysophosphatidic acid production.** *Semin Cell Dev Biol* 2004, **15**:477–489.
4. Kawagoe H, Stracke ML, Nakamura H, Sano K: **Expression and transcriptional regulation of the PD-Iα/autotaxin gene in neuroblastoma.** *Cancer Res* 1997, **57**:2516–2521.
5. Yang SY, Lee J, Park CG, Kim S, Hong S, Chung HC, Min SK, Han JW, Lee HW, Lee HY: **Expression of autotaxin (NPP-2) is closely linked to invasiveness of breast cancer cells.** *Clin Exp Metastasis* 2002, **19**:603–608.
6. Stassar MJ, Devitt G, Brosius M, Rinnab L, Prang J, Schradin T, Simon J, Petersen S, Kopp-Schneider A, Zöller M: **Identification of human renal cell carcinoma associated genes by suppression subtractive hybridization.** *Br J Cancer* 2001, **85**:1372–1382.
7. Umezu-Goto M, Kishi Y, Taira A, Hama K, Dohmae N, Takio K, Yamori T, Mills GB, Inoue K, Aoki J, Arai H: **Autotaxin has lysophospholipase D activity leading to tumor cell growth and motility by lysophosphatidic acid production.** *J Cell Biol* 2002, **158**:227–233.
8. Liu S, Umezu-Goto M, Murph M, Lu Y, Liu W, Zhang F, Yu S, Stephens LC, Cui X, Murrow G, Coombes K, Muller W, Hung MC, Perou CM, Lee AV, Fang X, Milles GB: **Expression of autotaxin and lysophosphatidic acid receptors**

increases mammary tumorigenesis, invasion, and metastases. *Cancer Cell* 2009, **15**:539–550. A published erratum appears in *Cancer Cell* 2009, **16**:172.
9. Masuda A, Nakamura K, Izutsu K, Igarashi K, Ohkawa R, Jona M, Higashi K, Yokota H, Okudaira S, Kishimoto T, Watanabe T, Koike Y, Ikeda H, Kozai Y, Kurokawa M, Aoki J, Yatomi Y: **Serum autotaxin measurement in haematological malignancies: a promising marker for follicular lymphoma.** *Br J Haematol* 2008, **143**:60–70.
10. Schleicher SM, Thotala DK, Linkous AG, Hu R, Leahy KM, Yazlovitskaya EM, Hallahan DE: **Autotaxin and LPA receptors represent potential molecular targets for the radiosensitization of murine glioma through effects on tumor vasculature.** *PLoS One* 2011, **6**:e22182.
11. Houben AJ, Moolenaar WH: **Autotaxin and LPA receptor signaling in cancer.** *Cancer Metastasis Rev* 2011, **30**:557–565.
12. Nikitopoulou I, Oikonomou N, Karouzakis E, Sevastou I, Nikolaidou-Katsaridou N, Zhao Z, Mersinias V, Armaka M, Xu Y, Masu M, Milles GB, Gay S, Kollias G, Aidinis V: **Autotaxin expression from synovial fibroblasts is essential for the pathogenesis of modeled arthritis.** *J Exp Med* 2012, **209**:925–933.
13. Kehlen A, Lauterbach R, Santos AN, Thiele K, Kabisch U, Weber E, Riemann D, Langner J: **IL-1β- and IL-4-induced down-regulation of autotaxin mRNA and PC-1 in fibroblast-like synoviocytes of patients with rheumatoid arthritis (RA).** *Clin Exp Immunol* 2001, **123**:147–154.
14. Bourgoin SG, Zhao C: **Autotaxin and lysophospholipids in rheumatoid arthritis.** *Curr Opin Investig Drugs* 2010, **11**:515–526.
15. Miyabe Y, Miyabe C, Iwai Y, Takayasu A, Fukuda S, Yokoyama W, Nagai J, Jona M, Tokuhara Y, Ohkawa R, Albers HM, Ovaa H, Aoki J, Chun J, Yatomi Y, Ueda H, Miyasaka M, Miyasaka N, Nanki T: **Necessity of lysophosphatidic acid receptor 1 for development of arthritis.** *Arthritis Rheum* 2013, **65**:2037–2047.
16. Cader MZ, Filer A, Hazlehurst J, de Pablo P, Buckley CD, Raza K: **Performance of the 2010 ACR/EULAR criteria for rheumatoid arthritis: comparison with 1987 ACR criteria in a very early synovitis cohort.** *Ann Rheum Dis* 2011, **70**:949–955.
17. Kaneko K, Miyabe Y, Takayasu A, Fukuda S, Miyabe C, Ebisawa M, Yokoyama W, Watanabe K, Imai T, Muramoto K, Terashima Y, Sugihara T, Matsushima K, Miyasaka N, Nanki T: **Chemerin activates fibroblast-like synoviocytes in patients with rheumatoid arthritis.** *Arthritis Res Ther* 2011, **13**:R158.
18. Watanabe K, Penfold ME, Matsuda A, Ohyanagi N, Kaneko K, Miyabe Y, Matsumoto K, Schall TJ, Miyasaka N, Nanki T: **Pathogenic role of CXCR7 in rheumatoid arthritis.** *Arthritis Rheum* 2010, **62**:3211–3220.
19. Tanaka M, Nakaide S, Takaoka Y: **Compounds having lysophosphatidic acid receptor antagonism and uses thereof.** Patent Version Number: WO/2005/058790 (2005-06-30) [http://patentscope.wipo.int/search/en/WO2005058790] (accessed 9 October 2014).
20. Ishii S, Noguchi K, Yanagida K: **Non-Edg family lysophosphatidic acid (LPA) receptors.** *Prostaglandins Other Lipid Mediat* 2009, **89**:57–65.
21. Bradfield PF, Amft N, Vernon-Wilson E, Exley AE, Parsonage G, Rainger GE, Nash GB, Thomas AM, Simmons DL, Salmon M, Buckley CD: **Rheumatoid fibroblast-like synoviocytes overexpress the chemokine stromal cell-derived factor 1 (CXCL12), which supports distinct patterns and rates of CD4+ and CD8+ T cell migration within synovial tissue.** *Arthritis Rheum* 2003, **48**:2472–2482.
22. Zhao C, Fernandes MJ, Prestwich GD, Turgeon M, Di Battista J, Clair T, Poubelle PE, Bourgoin SG: **Regulation of lysophosphatidic acid receptor expression and function in human synoviocytes: implications for rheumatoid arthritis?** *Mol Pharmacol* 2008, **73**:587–600.
23. Burger JA, Tsukada N, Burger M, Zvaifler NJ, Dell'Aquila M, Kipps TJ: **Blood-derived nurse-like cells protect chronic lymphocytic leukemia B cells from spontaneous apoptosis through stromal cell-derived factor-1.** *Blood* 2000, **96**:2655–2663.
24. Burger JA, Zvaifler NJ, Tsukada N, Firestein GS, Kipps TJ: **Fibroblast-like synoviocytes support B-cell pseudoemperipolesis via a stromal cell–derived factor-1– and CD106 (VCAM-1) –dependent mechanism.** *J Clin Invest* 2001, **107**:305–315.
25. Kanda H, Newton R, Klein R, Morita Y, Gunn MD, Rosen SD: **Autotaxin, an ectoenzyme that produces lysophosphatidic acid, promotes the entry of lymphocytes into secondary lymphoid organs.** *Nat Immunol* 2008, **9**:415–423.
26. Zhang Y, Chen YC, Krummel MF, Rosen SD: **Autotaxin through lysophosphatidic acid stimulates polarization, motility, and transendothelial migration of naive T cells.** *J Immunol* 2012, **189**:3914–3924.
27. Bai Z, Cai L, Umemoto E, Takeda A, Tohya K, Komai Y, Veeraveedu PT, Hata E, Sugiura Y, Kubo A, Suematsu M, Hayasaka H, Okudaira S, Aoki J, Tanaka T, Albers HM, Ovaa H, Miyasaka M: **Constitutive lymphocyte transmigration across the basal lamina of high endothelial venules is regulated by the autotaxin/lysophosphatidic acid axis.** *J Immunol* 2013, **190**:2036–2048.
28. Orosa B, González A, Mera A, Gómez-Reino JJ, Conde C: **Lysophosphatidic acid receptor 1 suppression sensitizes rheumatoid fibroblast-like synoviocytes to tumor necrosis factor-induced apoptosis.** *Arthritis Rheum* 2012, **64**:2460–2470.

doi:10.1186/s13075-014-0461-9
Cite this article as: Miyabe *et al.*: Activation of fibroblast-like synoviocytes derived from rheumatoid arthritis via lysophosphatidic acid–lysophosphatidic acid receptor 1 cascade. *Arthritis Research & Therapy* 2014 **16**:461.

ARTHRITIS & RHEUMATOLOGY
Vol. 66, No. 10, October 2014, pp 2751–2761
DOI 10.1002/art.38743

Macrophage-Derived Delta-like Protein 1 Enhances Interleukin-6 and Matrix Metalloproteinase 3 Production by Fibroblast-like Synoviocytes in Mice With Collagen-Induced Arthritis

Chiyoko Sekine,[1] Toshihiro Nanki,[2] and Hideo Yagita[3]

Objective. **We previously reported that blockade of the Notch ligand delta-like protein 1 (DLL-1) suppressed osteoclastogenesis and ameliorated arthritis in a mouse model of rheumatoid arthritis (RA). However, the mechanisms by which joint inflammation were suppressed have not yet been revealed. This study was undertaken to determine whether DLL-1 regulates the production of RA-related proinflammatory cytokines.**

Methods. **Joint cells from mice with collagen-induced arthritis (CIA) and mouse fibroblast-like synoviocytes (FLS) were cultured with or without stimuli in the presence of neutralizing antibodies against Notch ligands, and the production of proinflammatory cytokines was determined by enzyme-linked immunosorbent assay. The expression of Notch receptors and ligands on mouse joint cells was determined by flow cytometry.**

Results. **The production of interleukin-6 (IL-6) and granulocyte–macrophage colony-stimulating factor (GM-CSF) by mouse joint cells with or without stimulation was suppressed by DLL-1 blockade. DLL-1 blockade also suppressed the levels of IL-6 and matrix metalloproteinase 3 (MMP-3) in the joint fluid in a mouse model of RA. However, the production of tumor necrosis factor α and IL-1β was not suppressed by DLL-1 blockade. The production of IL-6 and MMP-3 by mouse FLS was enhanced by DLL-1 stimulation as well as Notch-2 activation. Among joint cells, DLL-1 was not expressed on mouse FLS but was expressed on macrophages.**

Conclusion. **These results suggest that the interaction of DLL-1 on mouse joint macrophages with Notch-2 on mouse FLS enhances the production of IL-6 and MMP-3. Therefore, suppression of IL-6, GM-CSF, and MMP-3 production by DLL-1 blockade might be responsible for the amelioration of arthritis in a mouse model of RA.**

Rheumatoid arthritis (RA) is a chronic autoimmune disease characterized by joint inflammation and synovial hyperplasia leading to joint destruction. At the site of inflammation, inflammatory cells, such as T cells, B cells, macrophages, and neutrophils, are recruited and further activated. These cells also activate joint cells, including fibroblast-like synoviocytes (FLS), chondrocytes, and osteoclasts, which increase inflammation and induce cartilage degradation and bone erosion (1).

The intimal lining of the synovium is composed of macrophage-like synoviocytes (type A synoviocytes) and FLS (type B synoviocytes) in relatively equal proportions. Macrophage-like synoviocytes express markers similar to other tissue resident macrophages, such as CD11b, CD68, CD14, and class II major histocompatibility antigens. They have little capacity to proliferate. FLS are mesenchymal cells that display many characteristics of fibroblasts and secrete proteins critical for joint lubrication, including hyaluronan and lubricin.

The synovium plays a key role in the pathogenesis of RA. Highly activated macrophage-like synoviocytes and FLS interact with each other directly and through the secretion of mediators that contribute to the perpetuation of synovitis and destruction of the extracellular

Supported by Grants-in-Aid from the Ministry of Education, Culture, Sports, Science, and Technology, Japan.

[1]Chiyoko Sekine, PhD: Juntendo University School of Medicine, Tokyo, Japan, and Teikyo University School of Medicine, Tokyo, Japan; [2]Toshihiro Nanki, MD, PhD: Teikyo University School of Medicine, Tokyo, Japan; [3]Hideo Yagita, PhD: Juntendo University School of Medicine, Tokyo, Japan.

Address correspondence to Chiyoko Sekine, PhD, Department of Immunology, Juntendo University School of Medicine, 2-1-1 Hongo, Bunkyo-ku, Tokyo 113-8421, Japan. E-mail: csekine@juntendo.ac.jp.

Submitted for publication September 16, 2013; accepted in revised form June 5, 2014.

matrix (1,2). The macrophage-like synoviocytes produce proinflammatory cytokines, chemokines, and growth factors, while the activated hyperplastic FLS augment destructive inflammation by producing cytokines, prostaglandins, proteases, and cartilage-degrading enzymes. Actually, these mediators are dominated in RA synovium, and FLS are the primary source of interleukin-6 (IL-6) and matrix metalloproteinases (MMPs) in RA. Moreover, FLS in RA exhibit unique aggressive features and exacerbate joint damage by invading the bone matrix of the rheumatoid joint.

It is well established that tumor necrosis factor α (TNFα) and IL-6 play dominant roles in the pathobiology of RA (1). IL-1 also has a significant impact on the disease process. Therapeutic use of agents that inhibit TNFα, IL-6, or IL-1 ameliorates inflammation and joint destruction in RA. Collagenases (MMP-1 and MMP-13) and stromelysin (MMP-3) are also important for the degradation of cartilage in RA (2). Their synthesis and activation are induced by various factors, including proinflammatory cytokines and Toll-like receptor ligands.

The Notch pathway is known to regulate cell fate decision and differentiation during embryonic and postnatal development (3). Notch is conserved across species, and 4 mammalian Notch receptors (Notch-1,- 2, -3, and -4) have been identified. Notch ligands of the delta-like protein (DLL) and Jagged families (DLL-1, DLL-4, Jagged-1, and Jagged-2) are transmembrane proteins, and the extracellular domain contains the Delta/Serrate/Lag-2 domain that is required for their interaction with Notch receptors. Jagged-1 and Jagged-2 contain an additional cysteine-rich domain. Receptor–ligand engagement triggers the cleavage of Notch receptor extracellular domain, which facilitates a cleavage within the Notch transmembrane domain by a γ-secretase. This leads to release of the Notch intracellular domain (ICD) from the membrane, and the released Notch ICD translocates to the nucleus to drive the expression of Notch target genes (3,4).

The importance of Notch receptors in osteoclast differentiation has been reported, and we previously found that DLL-1 promoted osteoclastogenesis via Notch-2, and that Jagged-1 suppressed osteoclastogenesis via Notch-1 in both mice and humans (5). We also demonstrated that DLL-1 blockade reduced the number of osteoclasts in the affected joints in a mouse model of RA and suppressed ovariectomy-induced bone loss in mice (5). In addition, the arthritis score and histologic examination of joint sections indicated the amelioration of arthritis by DLL-1 blockade in a mouse model of RA, suggesting that DLL-1 contributes to inflammation in the joint.

Involvement of Notch-1 in the TNFα-induced proliferation of RA synoviocytes has been demonstrated (6). Notch has also been implicated in vascular endothelial growth factor/angiopoietin 2–induced angiogenesis and the production of IL-6, IL-8, MMP-2, and MMP-9 in RA synovium (7,8). It has also been shown that Notch signal inhibitors suppressed IL-6 production by TNFα-stimulated FLS and by lipopolysaccharide (LPS)/interferon-γ (IFNγ)–stimulated macrophages (9,10). Notch signaling has also been implicated in cytokine production by dendritic cells and T cells (11,12). Therefore, DLL-1 could modulate the production of inflammatory cytokines in the mouse model of RA, underlying the suppression of joint inflammation by DLL-1 blockade demonstrated in our previous study (5). In the current study, we investigated whether DLL-1 regulates RA-related cytokine production in the joints in a mouse model of RA.

MATERIALS AND METHODS

Mice. Seven-week-old male DBA/1 mice were purchased from Charles River. Collagen-induced arthritis (CIA) was induced by immunization with 150 μg of bovine type II collagen (Collagen Research Center) emulsified with Freund's complete adjuvant (Difco) on day 0 and day 21. Eight weeks after the second immunization, peripheral blood (PB), spleen, bone marrow (BM), and joint cells were prepared and used for experiments. Mice with CIA were injected intraperitoneally with 0.25 mg of HMD1-5 or control hamster IgG twice a week for 2 weeks. Treatment was begun on day 21. Arthritis was assessed clinically by visual scoring using a scale of 0–4 as previously described (5). All animal experiments were approved by the Juntendo University Animal Experimental Ethics Committee.

Cell preparation. Mouse joint cells were prepared from the hind legs of mice with CIA 8 weeks after the second immunization, as previously described (13). Briefly, the skin was removed from the hind legs, soft tissue and tendons were cleaned as possible, and bones were then separated at the hip joint without damaging the bones, to avoid contamination with BM cells. The knee and ankle tendons were dissected in phosphate buffered saline containing 0.5 mg/ml of collagenase (Wako) to open up the joint cavity, then incubated at 37°C for 1 hour. Joint cells were pipetted from the knee and ankle joint spaces and subjected to red blood cell lysis.

To establish mouse FLS as previously described (14), joint cells prepared as described above were cultured in Dulbecco's modified Eagle's medium (DMEM; Wako) containing 10% fetal bovine serum (FBS; JRH Biosciences). Joint cells other than mouse FLS, including synovial macrophages, have a limited lifespan in vitro and rarely survive more than a few weeks in culture. Cells beyond the third passage were CD45-negative (99%). Cells from passages 6–11 were used.

Femoral BM cells from mice with CIA were cultured with 50 ng/ml of recombinant mouse macrophage colony-stimulating factor (M-CSF; Wako) in α-minimum essential medium (Wako) containing 10% FBS for 8 days and used as BM-derived macrophages (BMMs).

Antibodies. Generation and characterization of hamster IgG monoclonal antibodies (mAb) specific for mouse Notch-1 (HMN1-12), Notch-2 (HMN2-29), Notch-3 (HMN3-133), Notch-4 (HMN4-14), DLL-1 (HMD1-5), DLL-4 (HMD4-2), Jagged-1 (HMJ1-29), and Jagged-2 (HMJ2-1) have been described previously (15,16). The stimulating activity of the antireceptor mAb and the blocking activity of the antiligand mAb have been verified in vitro and in vivo (5,15,16). Fluorescein isothiocyanate (FITC)– or phycoerythrin (PE)–labeled mAb against mouse CD45 (30-F11), PerCP–Cy5.5–labeled mAb against mouse CD11b (M1/70), allophycocyanin-labeled mAb against mouse F4/80 (BM8), and PE-conjugated streptavidin were obtained from eBioscience. FITC-labeled mAb against mouse Ly6G (1A8) was from BD Bioscience. Antibodies against cleaved Notch-1 (Val1744) and α-tubulin (11H10) were purchased from Cell Signaling Technology. Antibody specific for Notch-2 ICD (411801) was from R&D Systems.

Reagents. The γ-secretase inhibitor DAPT was purchased from Calbiochem and used at 10 μM. Recombinant mouse TNFα and IL-1β were purchased from Wako and used at 10 ng/ml. Recombinant mouse IFNγ (Wako) was used at 50 ng/ml, and LPS (Sigma) was used at 10 ng/ml.

Flow cytometry. Multicolor staining was conducted using combinations of the indicated mAb as previously described (16). The cells were analyzed on a FACSCalibur system and analyzed with CellQuest software (both from BD Biosciences).

Cell culture. Mouse joint cells (3×10^5/ml) or mouse FLS (5×10^4/ml) were cultured in DMEM containing 10% FBS in the presence of the indicated reagents. Cytokine concentrations in the culture supernatant were measured using a specific enzyme-linked immunosorbent assay (ELISA) kit according to the protocols recommended by the manufacturers (OptEIA for TNFα, IL-1β, and IL-6 [BD Biosciences] and Quantikine for MMP-3 and GM-CSF [R&D Systems]). Cell viability was accessed by water-soluble tetrazolium 8 assay using Cell Counting Kit 8 (Dojin).

Chinese hamster ovary (CHO) cells and mouse DLL-1–, DLL-4–, Jagged-1–, or Jagged-2–transfected cells (15) were fixed with 1% paraformaldehyde, then used as stimulators. Mouse FLS were cultured with 10 μM DAPT or control DMSO for 2 hours, then paraformaldehyde-fixed CHO transfectants were added in the presence or absence of 10 ng/ml LPS. Cytokine concentrations in the culture supernatant after 24 hours were measured by ELISA as described above.

To purify joint macrophages, CD11b+ cells were sorted from the joint cells of mice with CIA using CD11b MicroBeads (Miltenyi Biotec). These CD11b+ joint macrophages (3×10^5/ml) were cultured with mouse FLS (5×10^4/ml) for 24 hours, and cytokine concentrations were analyzed as described above. BMMs, developed as described above, were stimulated with IFNγ for 24 hours and then cultured with mouse FLS for 24 hours. Cytokine concentrations were analyzed as described above.

Joint fluid collection. Serum from arthritic K/BxN mice (100 μl) was injected into the peritoneal cavity of C57BL/6 mice on day 0 and day 2 to induce arthritis. Anti-mouse DLL-1 mAb (HMD1-5) or control hamster IgG (eBioscience) was administrated intraperitoneally twice a week, beginning on day 3. Arthritis scores and hematoxylin and eosin staining of the arthritic joints have been described previously (5). Thirteen days after serum transfer, the knee joints were opened from the patellar tendon and washed in 500 μl of complete medium, and incubated for 1 hour at room temperature to allow the elution of cytokines, as previously described (17). Supernatants were then removed and stored at −20°C until assayed. Joint fluid from mice with CIA was collected 36 days after immunization.

Immunohistochemistry. Joint cell suspensions were centrifuged onto glass cytospin slides, fixed with acetone, and then incubated with 2.5 μg/ml of rat anti-mouse IL-6 mAb (MP5-20F3; BD Bioscience) for 2 hours. They were then incubated with biotinylated antibody against rat immunoglobulins (DakoCytomation), and Alexa Fluor 594–labeled streptavidin (Molecular Probes) was used for detection. They were further incubated with FITC-labeled mAb to CD11b, then Alexa Fluor 488–labeled anti-FITC (Molecular Probes) was used as secondary antibody. DAPI was used for nuclear counterstain. Fluorescent images were acquired on a microscope (Eclipse TE300; Nikon) equipped with a digital camera (C10600-10B; Hamamatsu Photonics) and processed using AquaCosmos (Hamamatsu Photonics).

Paraffin-fixed joint tissue sections from mice with K/BxN serum–induced arthritis (described above) were deparaffinized, pretreated in Liberate Antibody Binding Solution (Polysciences) for 5 minutes, and incubated with 2.5 μg/ml of biotin-labeled HMD1-5. A Catalyzed Signal Amplification System and peroxidase (DakoCytomation) were used for detection. Color was developed with diaminobenzidine, whereas the sections were counterstained with hematoxylin. Images were acquired on a microscope (Eclipse E800M; Nikon) equipped with a digital camera (DS-Fi1c; Nikon) and processed using DS-L2 (Nikon). For fluorescence immunohistochemistry, HMD1-5 was detected using a Tyramide Signal Amplification Kit (PerkinElmer). To detect FITC-labeled mAb to CD11b, Alexa Fluor 488–labeled anti-FITC (Molecular Probes) was used as a secondary antibody. For staining CD248 (Abnova), biotinylated anti-rabbit IgG (Dako) was used as a secondary antibody and detected by Alexa Fluor 594–labeled streptavidin (Molecular Probes). Fluorescent images were acquired as described above.

Reverse transcriptase–polymerase chain reaction (RT-PCR). Total RNA was isolated using TRIzol reagent (Life Technologies) and was reverse-transcribed to complementary DNA with oligo(dT) and SuperScript RT (Invitrogen). PCR consisted of 35 cycles of 45 seconds at 94°C, 1 minute at 58°C, and 1 minute at 72°C. The primers have been described previously (5).

Immunoblotting. Immunoblotting was performed as previously described (5). Briefly, mouse FLS were lysed in whole cell lysis buffer (20 mM HEPES, pH 7.8, 420 mM NaCl, 0.5% Nonidet P40, 25% glycerol, 0.2 mM EDTA, 1.5 mM $MgCl_2$, 1 mM dithiothreitol, 1 mM phenylmethylsulfonyl fluo-

ride, and complete protease inhibitors) (Roche). The lysates were subjected to sodium dodecyl sulfate–polyacrylamide gel electrophoresis and transferred to PVDF membranes. These membranes were incubated with primary antibody, and then with horseradish peroxidase–conjugated secondary antibodies. The immunoreactive proteins were visualized using ECL Prime (GE Healthcare).

RNA interference. Small interfering RNAs (siRNAs) targeting mouse Notch-1 or Notch-2 and scrambled negative control siRNA were purchased from OriGene. Each siRNA was transfected into mouse FLS using Metafectene Pro (Biontex). Cell surface expression was analyzed by flow cytometry to validate the silencing of Notch-1 or Notch-2.

Statistical analysis. All comparisons between 2 groups were analyzed using Student's unpaired *t*-test. *P* values less than 0.05 were considered significant.

RESULTS

Mouse joint cell populations. Joint cells were prepared from the arthritic hind legs of mice with CIA as described in Materials and Methods. As shown in Figure 1A, CD45−CD11b− cells, which included mouse FLS, were detected in joint cells but few were detected in PB or BM cells. In contrast, the CD45+CD11b− cell population, mainly CD3+B220− T and CD3−B220+ B lymphocytes, was small in joint cells but abundant in PB cells. In the CD45+CD11b^{high} cell population, Ly6G^{high}F4/80− neutrophils were detected in similar percentages in joint, PB, and BM cells. While joint cells had Ly6G^{intermediate}F4/80^{high} tissue-resident macrophages, PB and BM cells had Ly6G−F4/80^{intermediate} monocyte-lineage cells in the CD45+CD11b^{high} compartment. As expected, the number of joint cells obtained from normal mice was 14 times lower than that obtained from mice with CIA, and few leukocytes were detected in normal joint cells (Figure 1B). The increase in neutrophils was most prominent in joint cells from mice with CIA, but the macrophage population and the fibroblast population were also increased considerably.

DLL-1 blockade suppresses IL-6 production by mouse joint cells. To address how the blockade of DLL-1 suppressed joint inflammation in K/BxN serum–transfer arthritis (5), a mouse model of RA (18,19), we determined the effect of DLL-1 blockade on the production of RA-related proinflammatory cytokines in a culture of mouse joint cells. Production of TNFα and IL-1β was not affected by the blockade of DLL-1, DLL-4, Jagged-1, or Jagged-2 (Figure 2A). Production of IL-6, GM-CSF, and MMP-3 was significantly suppressed by the blockade of DLL-1 but not DLL-4, Jagged-1, or Jagged-2 (Figure 2A). The production of IL-6, GM-CSF, and MMP-3 by mouse joint cells was enhanced by stimulation with TNFα and IL-1β, and this increase was also suppressed by DLL-1 blockade, while cell viability was not reduced (Figure 2B). IL-6 and GM-CSF production by LPS-stimulated mouse spleen cells was also suppressed by DLL-1 blockade, while TNFα and IL-1β levels were not affected (Figure 2C). MMP-3 production from LPS-stimulated spleen cells was not detected. These results indicate that the contri-

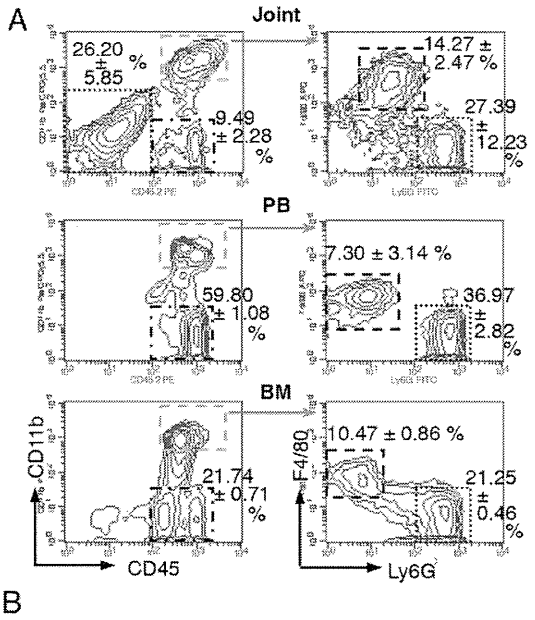

B

Joint cell populations	CIA	Normal
Total	4560 ± 611	320 ± 11
CD45$^-$CD11b$^-$Ly6G$^-$F4/80$^-$ (Fibroblasts)	1140 ± 115	138 ± 86
CD45$^+$CD11b^{hi}Ly6G^{int}F4/80^{hi} (Macrophages)	640 ± 128	26 ± 8
CD45$^+$CD11b^{hi}Ly6G^{hi}F4/80$^-$ (Neutrophils)	1080 ± 383	23 ± 17
CD45$^+$CD11b$^-$CD3$^+$B220$^-$ (T lymphocytes)	120 ± 38	7 ± 2
CD45$^+$CD11b$^-$CD3$^-$B220$^+$ (B lymphocytes)	190 ± 75	14 ± 1

Figure 1. Cell populations in the joints of mice with collagen-induced arthritis (CIA). **A,** Flow cytometric analysis of populations of joint cells, peripheral blood (PB), and bone marrow (BM) cells from mice with CIA. Right panels show staining of the CD45+CD11b^{high}-gated cells in the left panels. Values are the mean ± SD percent of total cells (n = 3 mice). **B,** Results of flow cytometric analysis of joint cell populations from mice with CIA and normal mice. Values are the mean ± SD cell number (× 10^2) per leg (n = 3 mice per group).

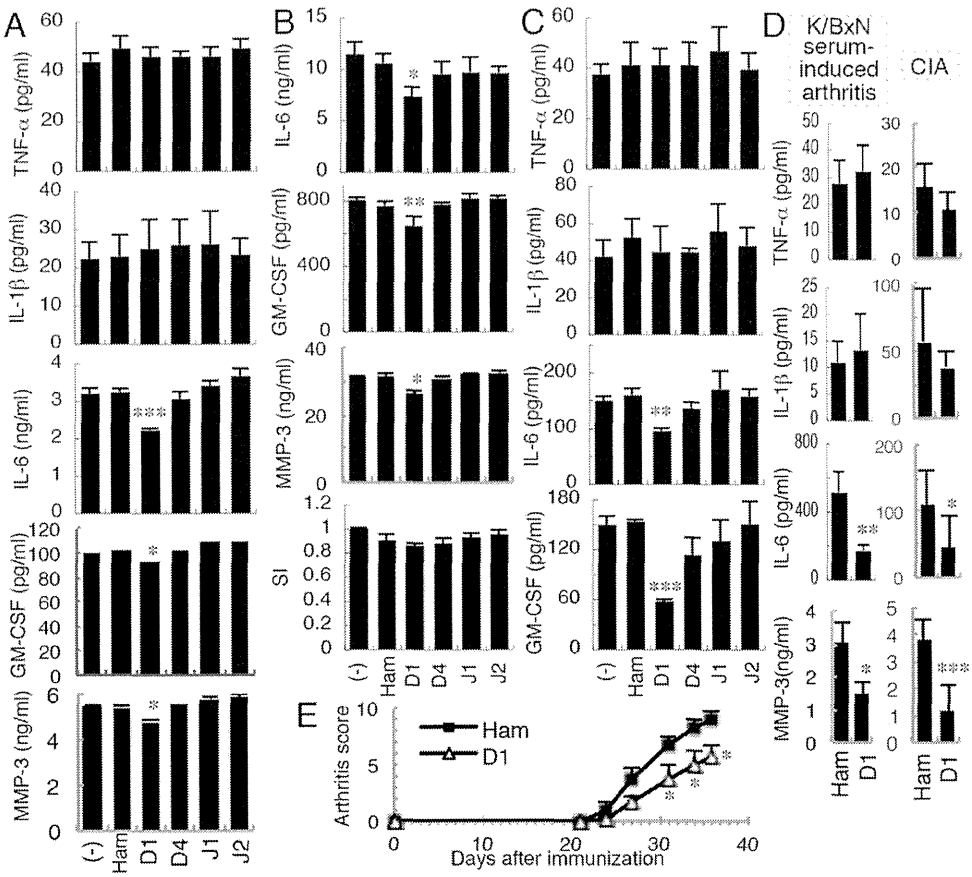

Figure 2. Effects of Notch ligand blockade on inflammatory cytokine production by joint cells from mice with collagen-induced arthritis (CIA). **A,** Levels of cytokines in the supernatants of joint cells from mice with CIA after 24 hours of culture with 20 μg/ml of the indicated monoclonal antibody (mAb) (HMD1-5 [D1], HMD4-2 [D4], HMJ1-29 [J1], or HMJ2-1 [J2]) or control hamster IgG (Ham), as measured by enzyme-linked immunosorbent assay (ELISA). **B,** Levels of cytokines in the supernatants of joint cells from mice with CIA after 24 hours of stimulation with tumor necrosis factor α (TNFα) and interleukin-1β (IL-1β) (10 ng/ml each) in the presence of the indicated mAb or control, as measured by ELISA. Cell viability was analyzed by water-soluble tetrazolium 8 assay and is indicated as the stimulation index (SI). **C,** Levels of cytokines in the supernatants of spleen cells from mice with CIA after 24 hours of stimulation with 10 ng/ml lipopolysaccharide in the presence of the indicated mAb or control, as measured by ELISA. In **A–C,** values are the mean ± SD from triplicate wells. **D,** Cytokines in the joint fluid of mice with K/BxN serum–induced arthritis and mice with CIA treated with control hamster IgG or HMD1-5, as measured by ELISA. Values are the mean ± SD (n = 7 mice per group). **E,** Severity of arthritis, assessed by arthritis score, in mice with CIA treated with control hamster IgG or HMD1-5. Values are the mean ± SEM (n = 7 mice per group). In **A–E,** results are representative of 3 independent experiments. * = $P < 0.05$; ** = $P < 0.01$; *** = $P < 0.001$ versus control hamster IgG. GM-CSF = granulocyte–macrophage colony-stimulating factor; MMP-3 = matrix metalloproteinase 3.

bution of DLL-1 to IL-6 and GM-CSF production is not specific to the mouse joint cells.

Next, we measured the levels of TNFα, IL-1β, IL-6, GM-CSF, and MMP-3 in the sera and swollen joints of mice with K/BxN serum–induced arthritis that were treated with anti–DLL-1 mAb or control IgG as previously described (5). Although these cytokines were undetectable in the serum on day 13, the levels of IL-6 and MMP-3, but not TNFα or IL-1β, in the joints of anti–DLL-1 mAb–treated mice were significantly lower than those in the control IgG-treated mice (Figure 2D). The levels of IL-6 and MMP-3 in the joint fluid of mice with CIA were also suppressed by anti–DLL-1 mAb treatment (Figure 2D). GM-CSF was undetectable in the joints of these mice. In addition, in mice with CIA, arthritis was suppressed by DLL-1 blockade (Figure 2E). These results suggest that the suppression of IL-6, GM-CSF, and MMP-3 production in the mouse joint might be responsible for the suppression of arthritis by DLL-1 blockade.

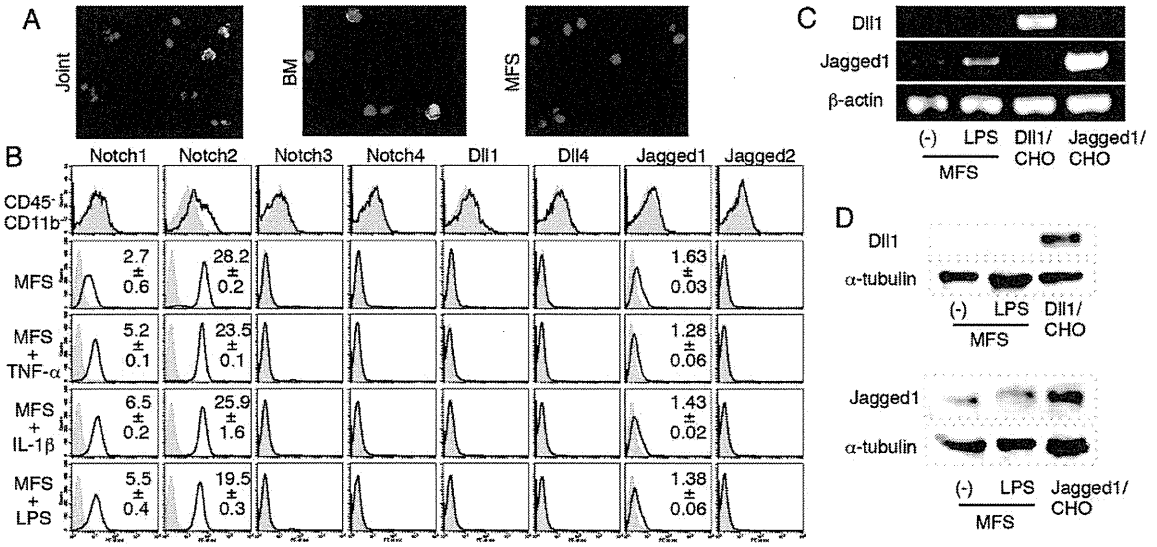

Figure 3. Mouse fibroblast-like synoviocyte (FLS) expression of Notch receptors and ligands. **A,** Immunohistologic staining of joint cells, bone marrow (BM) cells, and FLS (MFS) from mice with CIA. Green indicates CD11b, red indicates IL-6, and blue indicates DAPI. Original magnification × 200. **B,** Expression of Notch receptors and ligands on CD45−CD11b− mouse joint cells, analyzed by flow cytometry. Mouse FLS were cultured with or without the indicated stimulus for 6 hours, and then expression was analyzed. Shaded histograms indicate staining with control hamster IgG. Open histograms indicate staining with mAb specific for the indicated Notch receptor or ligand. Values are the mean ± SD mean fluorescence intensity of positive staining divided by control (n = 3 independent experiments). **C,** Levels of mRNA for delta-like protein 1 (DLL-1) and Jagged-1, measured by reverse transcriptase–polymerase chain reaction. Mouse FLS were cultured with or without lipopolysaccharide (LPS) for 6 hours. DLL-1–transfected Chinese hamster ovary (CHO) cells and Jagged-1–transfected CHO cells were used as positive controls. **D,** Western blotting of DLL-1 and Jagged-1 using HMD1-5 (for DLL-1) or HMJ1-29 (for Jagged-1). Mouse FLS were cultured with or without LPS for 6 hours. DLL-1–transfected CHO cells and Jagged-1–transfected CHO cells were used as positive controls, and α-tubulin was used as a loading control. See Figure 2 for other definitions.

Expression of Notch receptors and ligands by mouse FLS. The mouse joint cells produced a high level of IL-6, while levels of TNFα and IL-1β were low (Figure 2A). We found that IL-6 was produced by a subset of CD11b− nonmyeloid cells in the joints and cultured mouse FLS, while CD11b+ macrophages in the joint and BM did not secrete IL-6 (Figure 3A). IL-6 production by cultured BM cells was not detectable by ELISA (data not shown). Therefore, we next examined whether DLL-1 was involved in the production of IL-6 by mouse FLS.

As shown in Figure 3B, the CD45−CD11b− FLS population in the joint cells expressed Notch-2, and low levels of DLL-1 and Jagged-1 were also detected. Mouse FLS, which were established as described in Materials and Methods, also expressed Notch-2 and Jagged-1 but not DLL-1. Notch-1 expression was detected on mouse FLS and was up-regulated significantly by inflammatory stimulation with TNFα, IL-1β, or LPS ($P = 0.00031$, $P = 0.000029$, and $P = 0.000018$, respectively). In contrast, Notch-2 and Jagged-1 expression on mouse FLS were slightly down-regulated by such stimulation. Statistical analysis showed that these decreases in expression were also significant ($P = 0.0005$ for TNFα, $P = 0.027$ for IL-1β, and $P = 0.00025$ for LPS). DLL-1 expression on mouse FLS was not detectable even after stimulation. RT-PCR analysis showed that DLL-1 messenger RNA (mRNA) was not detectable in mouse FLS with or without LPS stimulation, while Jagged-1 mRNA was expressed in mouse FLS (Figure 3C). Immunoblot analysis supported these results, indicating that DLL-1 was not detectable, while Jagged-1 was expressed in mouse FLS (Figure 3D).

Enhanced production of IL-6 and MMP-3 by mouse FLS cultured with DLL-1. Since DLL-1 was not detected on mouse FLS, DLL-1 on other cells in the joints could stimulate Notch-1 and Notch-2 on mouse FLS. As shown in Figure 4A, IL-6 production by mouse FLS was enhanced by DLL-1 but not by any other Notch ligands. Levels of MMP-3, which is produced primarily

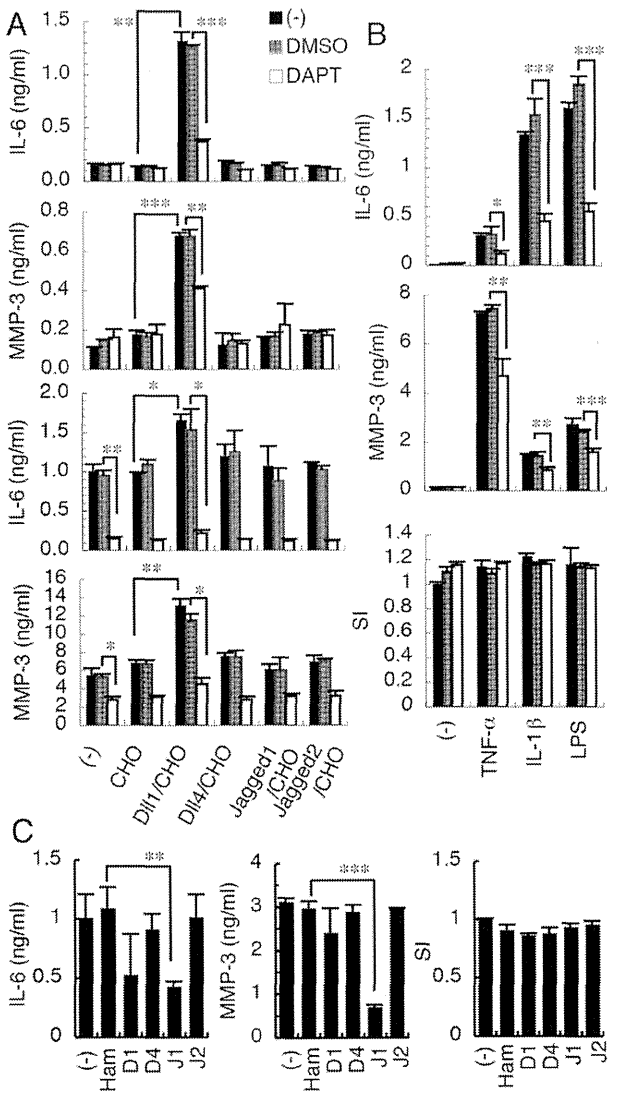

Figure 4. Increased production of IL-6 and MMP-3 by fibroblast-like synoviocytes (FLS) from mice with CIA cultured with delta-like protein 1 (DLL-1). **A,** Levels of IL-6 and MMP-3 in mouse FLS cultured with DLL-1–, DLL-4–, Jagged-1–, or Jagged-2–transfected Chinese hamster ovary (CHO) cells or control CHO cells in the presence of DAPT or DMSO control for 24 hours, as measured by ELISA. The 2 bottom panels show the results of experiments that also included stimulation with lipopolysaccharide (LPS). **B,** Levels of IL-6 and MMP-3 in mouse FLS cultured with the indicated stimulus for 24 hours in the presence of DAPT or DMSO control, as measured by ELISA. Cell viability was analyzed by water-soluble tetrazolium 8 assay and is indicated as the SI. **C,** Levels of IL-6 and MMP-3 in mouse FLS stimulated with LPS in the presence of the indicated mAb or control hamster IgG as described in Figure 1, as measured by ELISA. Results are representative of 3 independent experiments. Values are the mean ± SD from triplicate wells. * = $P < 0.05$; ** = $P < 0.01$; *** = $P < 0.001$. See Figure 2 for other definitions.

by FLS and is important for cartilage degradation in RA, were also increased by DLL-1. This enhancement by DLL-1 was abrogated by the Notch inhibitor DAPT, implying that DLL-1 activates Notch signaling. Stimulation of mouse FLS with LPS up-regulated the production of IL-6 and MMP-3, and DLL-1 further enhanced it (Figure 4A). The LPS-induced up-regulation, as well as the DLL-1–induced enhancement, was also abrogated by DAPT (Figure 4A), indicating that the LPS-induced up-regulation was also Notch dependent. In addition, TNFα-induced and IL-1β–induced up-regulation of IL-6 and MMP-3 was inhibited by DAPT, while cell viability was not affected (Figure 4B). These results imply that Notch signaling via mouse FLS–mouse FLS interactions is involved in the up-regulation of IL-6 and MMP-3 by these proinflammatory agents. Consistent with the expression of Notch ligands on mouse FLS (Figures 3B–D), blockade of Jagged-1 only inhibited the IL-6 and MMP-3 production by LPS-stimulated mouse FLS without affecting cell viability (Figure 4C). Production of GM-CSF by mouse FLS was undetectable even with stimulation in this culture condition (data not shown).

Expression of DLL-1 on mouse joint cells. Since DLL-1 was involved in the production of IL-6 by mouse FLS, we next determined the DLL-1–expressing cells in the joint. As shown in Figure 5A, DLL-1 was expressed on $CD11b^{high}Ly6G^{intermediate}F4/80^{high}$ macrophages but not on $CD11b^{high}Ly6G^{high}F4/80-$ neutrophils or CD45+CD11b− lymphocytes. Notch-2 was expressed on all of these cells. DLL-1 was also expressed on the $CD11b^{high}Ly6G-F4/80^{intermediate}$ monocyte/macrophage population in the PB and BM of arthritic mice (Figure 5B).

To examine the effect of inflammation on DLL-1 expression on macrophages, BMMs were stimulated with inflammatory cytokines. BMMs expressed DLL-1 at a low level (mean ± SD MFI 1.33 ± 0.049), and the expression was strongly up-regulated by IFNγ stimulation (mean ± SD MFI 7.21 ± 1.16; $P = 0.00091$), while TNFα or IL-1β stimulation had no effect (Figure 5C). Stimulation of BMMs with a combination of TNFα and IL-1β also did not affect the expression of Notch ligands (data not shown). Expression of Jagged-1 and Jagged-2 was also up-regulated by IFNγ (for Jagged-1, mean ± SD MFI 1.13 ± 0.025 versus 1.91 ± 0.14; $P = 0.00063$ and for Jagged-2, mean ± SD MFI 3.97 ± 0.39 versus 7.52 ± 0.70; $P = 0.0016$) (Figure 5C).

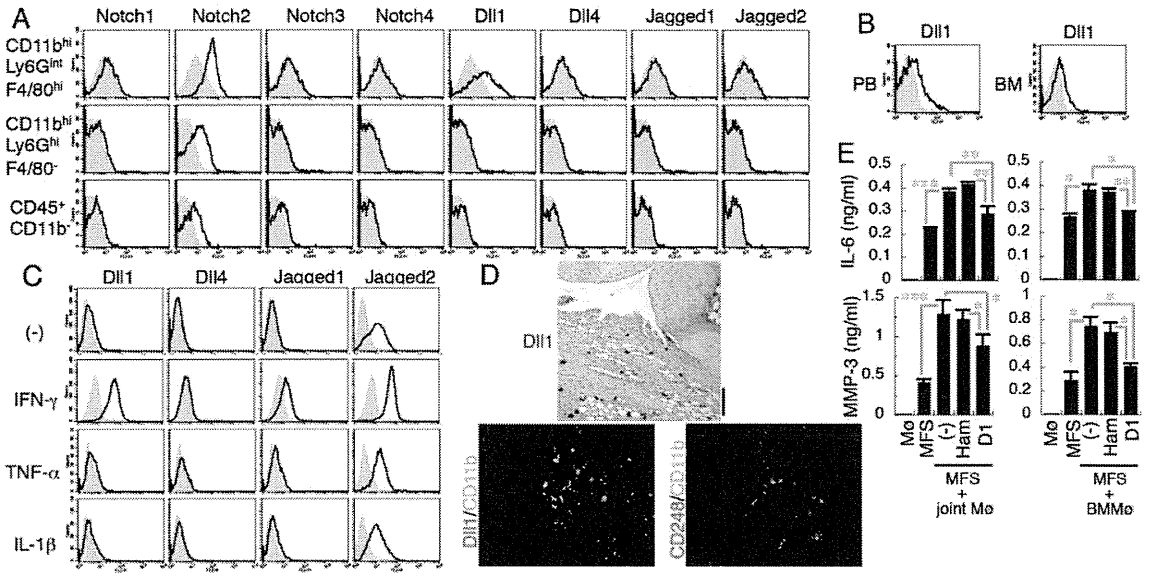

Figure 5. Expression of Notch receptors and ligands on macrophages (Mϕ). **A,** Expression of Notch receptors and ligands on the indicated joint cell populations from mice with CIA, analyzed by flow cytometry. **B,** Delta-like protein 1 (DLL-1) expression by the monocyte/macrophage population ($CD11b^{high}Ly6G-F4/80^{intermediate}$) in bone marrow (BM) and peripheral blood (PB) from mice with CIA. **C,** Expression of Notch ligands on BM-derived macrophages (BMMs). BMMs were stimulated with the indicated cytokine for 24 hours, and the expression of Notch ligands was analyzed by flow cytometry. In **A–C,** shaded histograms indicate staining with control hamster IgG, and open histograms indicate staining with mAb specific for the indicated Notch receptor or ligand. **D,** Immunohistochemical staining for DLL-1 expression in arthritic joints from mice with K/BxN serum–induced arthritis. Representative staining is shown. Bar = 100 μm in top panel. Original magnification × 200 in bottom panels. **E,** Levels of IL-6 and MMP-3 in the supernatants of fibroblast-like synoviocytes (MFS) from mice with CIA cultured with CD11b+ cells (macrophages) sorted from the joints of mice with CIA (left) or cultured with interferon-γ (IFNγ)–stimulated BMMs (right), as measured by ELISA. Cells were cultured in the presence of HMD1-5 or control hamster IgG. Results are representative of 3 independent experiments. Values are the mean ± SD from triplicate wells. * = $P < 0.05$; ** = $P < 0.01$; *** = $P < 0.001$. See Figure 2 for other definitions.

DLL-1 expression in the joints of arthritic mice was determined by immunohistochemistry (Figure 5D). Double-labeling of arthritic joints revealed that some of the CD11b+ cells expressed DLL-1 and were in direct contact with CD248+ mouse FLS (13) (Figure 5D). To verify that the interaction of macrophages and mouse FLS induced IL-6 and MMP-3 production, CD11b+ cells in the joints were isolated and cultured with established mouse FLS. As shown in Figure 5E, stimulation of mouse FLS with CD11b+ joint cells enhanced the production of IL-6 and MMP-3, and these increases were suppressed by DLL-1 blockade. Consistent with the results shown in Figure 3A, IL-6 was not secreted from CD11b+ joint cells alone (Figure 5E). Stimulation of mouse FLS with IFNγ-stimulated BMMs, which expressed DLL-1 as shown in Figure 5C, also enhanced the production of IL-6 and MMP-3, and these increases were inhibited by DLL-1 blockade (Figure 5E).

Notch-2 signaling enhances the production of IL-6 and MMP-3 by mouse FLS. Although Notch-1 and Notch-2 were expressed on mouse FLS (Figure 3B), production of IL-6 and MMP-3 was enhanced only by anti–Notch-2 agonistic mAb with or without LPS stimulation (Figures 6A and B). GM-CSF production was undetectable with such stimulation (data not shown). Stimulation of Notch-1 and Notch-2 with each agonistic mAb was demonstrated by induction of Notch-1 ICD and Notch-2 ICD, respectively (Figure 6C). Notably, LPS stimulation of mouse FLS preferentially induced Notch-2 ICD, and DAPT suppressed this generation of Notch-2 ICD as well as Notch-1 ICD (Figure 6C). Furthermore, stimulation of mouse FLS with DLL-1 induced Notch-2 ICD but not Notch-1 ICD (Figure 6D). In addition, the specific inhibition of Notch-2, but not that of Notch-1, in mouse FLS using siRNA resulted in a decrease in IL-6 and MMP-3 production, while cell viability was equivalent (Figure 6E). These results indi-

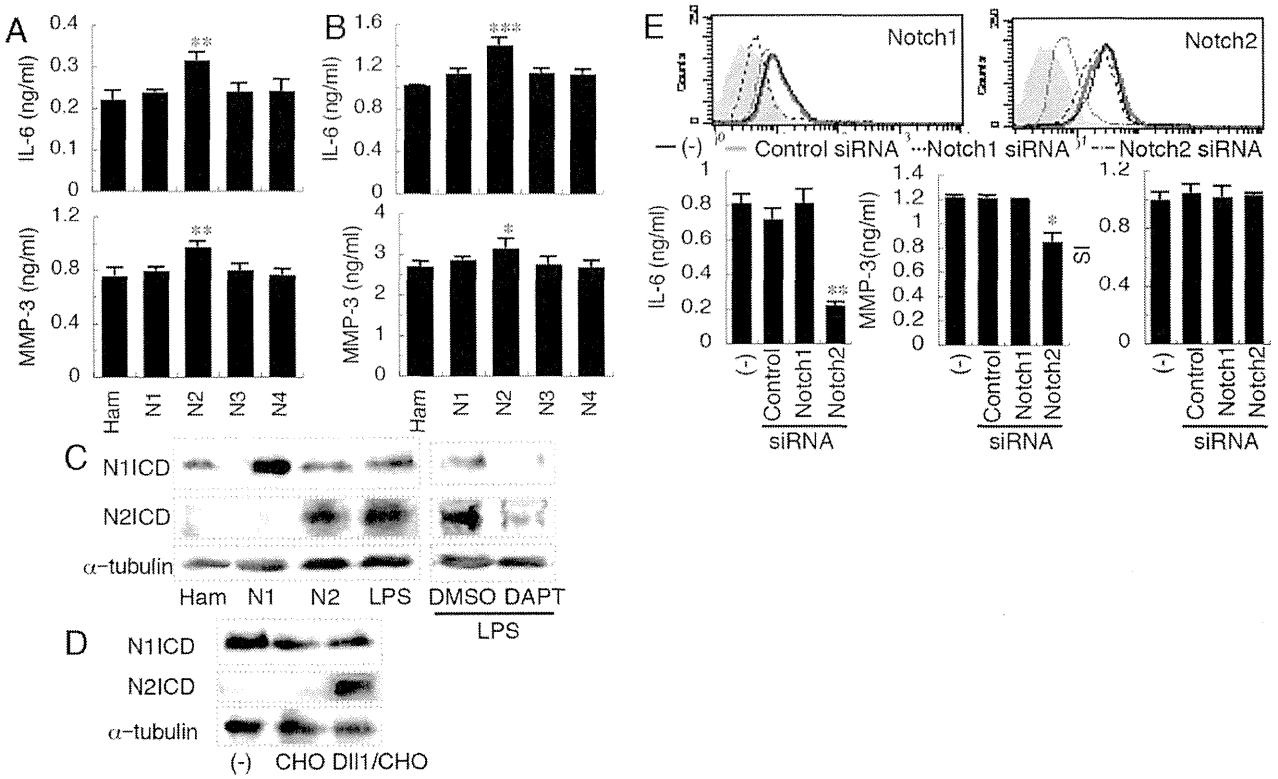

Figure 6. Notch-2 activation enhances IL-6 and MMP-3 production by fibroblast-like synoviocytes (FLS) from mice with CIA. **A** and **B,** Levels of IL-6 and MMP-3 in the supernatants of mouse FLS stimulated with 5 μg/ml of immobilized mAb (HMN1-12 [N1], HMN2-29 [N2], HMN3-133 [N3], or HMN4-14 [N4]) or control hamster IgG for 24 hours in the absence (**A**) or presence (**B**) of lipopolysaccharide (LPS). IL-6 and MMP-3 levels were measured by ELISA. Values are the mean ± SD from triplicate wells. * = $P < 0.05$; ** = $P < 0.01$; *** = $P < 0.001$, versus control hamster IgG. **C** and **D,** Western blot analysis of the Notch-1 intracellular domain (N1ICD) and Notch-2 ICD in mouse FLS cultured with the indicated mAb or LPS in the presence of DAPT or DMSO control (**C**), or with paraformaldehyde-fixed delta-like protein 1 (DLL-1)–transfected Chinese hamster ovary (CHO) cells or control CHO cells (**D**) for 15 hours. The loading control was α-tubulin. Results are representative of 3 independent experiments. **E,** Levels of IL-6 and MMP-3 in mouse FLS after inhibition of Notch-1 and Notch-2. Notch-1 small interfering RNA (siRNA) or Notch-2 siRNA was transfected into mouse FLS. Expression of Notch-1 and Notch-2 was analyzed by flow cytometry to validate the reduction. Shaded histograms indicate control hamster IgG staining. Open histograms indicate Notch-1 or Notch-2 mAb staining. Transfected siRNA are indicated for each histogram. Mouse FLS transfected with the indicated siRNA were stimulated with LPS. IL-6 and MMP-3 were measured as described in **A**. Cell viability is indicated as the SI. * = $P < 0.05$; ** = $P < 0.01$, versus control. See Figure 2 for other definitions.

cate that Notch-2 signaling enhances the production of IL-6 and MMP-3 by mouse FLS.

DISCUSSION

We previously reported that DLL-1 blockade ameliorates the arthritis induced by K/BxN serum transfer in mice, and histologic examination indicated that DLL-1 blockade suppressed inflammation in the joint in addition to suppressing osteoclastogenesis (5). To examine how DLL-1 blockade suppressed joint inflammation, we investigated whether DLL-1 regulates the production of RA-related proinflammatory cytokines in the mouse joint.

In this study, we demonstrated that stimulation of mouse FLS with DLL-1 enhanced the production of IL-6 and MMP-3. Notch-2 signaling also enhanced the production of IL-6 and MMP-3 by mouse FLS, and DLL-1 stimulation activated Notch-2 signaling in mouse FLS. These results indicate that DLL-1 promotes the production of IL-6 and MMP-3 by mouse FLS via Notch-2. In these experiments, strong expression of DLL-1 on DLL-1–transfected CHO cells (15)

activated Notch-2 vigorously, while the agonistic effect of HMN2-29 mAb to activate Notch-2 was weaker than the effect of the ligand. We also found that DLL-1 blockade suppressed the production of IL-6 and MMP-3 by joint cells from arthritic mice in vitro and in vivo. DLL-1 was expressed on joint macrophages, and the expression of DLL-1 on BMMs was up-regulated by IFNγ. This was consistent with our previous report that IFNγ induced DLL-1 expression on thioglycolate-elicited peritoneal macrophages (15). Of note, IFNγ did not induce the expression of DLL-1, or of DLL-4, Jagged-1, or Jagged-2, on mouse FLS (data not shown). IFNγ is produced by Th1 cells, CD8 T cells, and natural killer cells and is involved in arthritis. Collectively, DLL-1 on macrophages in the joint, which was up-regulated by IFNγ, could activate Notch-2 on mouse FLS, leading to the production of IL-6 and MMP-3. Therefore, DLL-1 blockade might ameliorate inflammation in the joint by suppressing the production of IL-6 and MMP-3 by mouse FLS.

In RA, blockade of IL-6 with biologic agents improves clinical outcomes, but K/BxN serum transfer resulted in comparable arthritis in IL-6–deficient mice and control mice (20), suggesting that suppression of IL-6 alone might not be sufficient to suppress K/BxN serum–induced arthritis. However, DLL-1 blockade also suppressed GM-CSF production. GM-CSF is important for the activation, differentiation, and survival of neutrophils and macrophages. Blockade of GM-CSF has been effective against RA in clinical trials (21). It has been reported that GM-CSF blockade ameliorated K/BxN serum–induced arthritis by regulating systemic and joint myeloid cell populations (22). Since DLL-1 was expressed on joint macrophages, macrophage–macrophage interactions may contribute to the GM-CSF production by Notch activation in the joint. Further studies are needed to address this possibility.

Notch-1 signaling was not involved in the production of IL-6 and MMP-3 by mouse FLS, while the expression was up-regulated by proinflammatory stimuli. DLL-1 stimulation did not activate Notch-1 signaling in mouse FLS, suggesting that Notch-1 on mouse FLS was not involved in the enhancement of arthritis by DLL-1. A preferential interaction of Notch-2 with DLL-1 has been reported in marginal zone B cell development (3) and osteoclastogenesis (5). Notch-1 was also expressed on these cells. Glycosylation of Notch extracellular domain by Fringe regulates DLL–Notch interactions (23–25). Therefore, a differential modification of Notch-1 and Notch-2 on mouse FLS by Fringe might be responsible for the preferential interaction of Notch-2–DLL-1. It would be interesting to elucidate whether Notch-1 on mouse FLS plays any role in arthritis.

Jagged-1 was the only Notch ligand that was expressed on mouse FLS, and Jagged-1 blockade, as well as Notch inhibitor, suppressed IL-6 and MMP-3 production by LPS-stimulated mouse FLS, indicating that Jagged-1 on mouse FLS stimulates Notch receptors on mouse FLS to produce these mediators. However, stimulation of mouse FLS with Jagged-1–transfected CHO cells did not enhance the production of these mediators, and the blockade of Jagged-1 did not suppress cytokine production by joint cells. Therefore, Jagged-1 could regulate IL-6 and MMP-3 production through mouse FLS–mouse FLS interactions but may play little role in total joint cells. The mechanism to explain this discrepancy remains to be determined.

The effect of DLL-1 blockade on LPS-stimulated mouse spleen cells suggests a systemic regulation of these cytokines by DLL-1 blockade. It is also intriguing to investigate whether IL-6, GM-CSF, and MMP-3 are direct target genes of Notch-2 ICD, but not Notch-1 ICD. The up-regulation of DLL-1 on macrophages by IFNγ seems to enhance the production of IL-6, MMP-3, and GM-CSF in the mouse joint, leading to augmentation of joint inflammation. The clinical relevance to human RA is now under investigation, but preliminary results demonstrated that IL-6 production by RA FLS was suppressed by DAPT, and RA FLS expressed Notch-2 and Jagged-1 but not Notch-1, as in mice (data not shown). Therefore, DLL-1 blockade may be a novel strategy to treat RA by suppressing not only osteoclastogenesis but also inflammatory cytokine production in the joint.

AUTHOR CONTRIBUTIONS

All authors were involved in drafting the article or revising it critically for important intellectual content, and all authors approved the final version to be published. Dr. Sekine had full access to all of the data in the study and takes responsibility for the integrity of the data and the accuracy of the data analysis.

Study conception and design. Sekine, Yagita.
Acquisition of data. Sekine, Nanki.
Analysis and interpretation of data. Sekine, Yagita.

REFERENCES

1. Choy E. Understanding the dynamics: pathways involved in the pathogenesis of rheumatoid arthritis. Rheumatology (Oxford) 2012;51:v3–11.
2. Bartok B, Firestein G. Fibroblast-like synoviocytes: key effector cells in rheumatoid arthritis. Immunol Rev 2010;233:233–55.
3. Radtke F, Fasnacht N, Macdonald HR. Notch signaling in the immune system. Immunity 2010;32:14–27.

4. Hori K, Sen A, Artavanis-Tsakonas S. Notch signaling at a glance. J Cell Sci 2013;126:2135–40.
5. Sekine C, Koyanagi A, Koyama N, Hozumi K, Chiba S, Yagita H. Differential regulation of osteoclastogenesis by Notch2/Delta-like 1 and Notch1/Jagged1 axes. Arthritis Res Ther 2012;14:R45.
6. Nakazawa M, Ishii H, Aono H, Takai M, Honda T, Aratani S, et al. Role of Notch-1 intracellular domain in activation of rheumatoid synoviocytes. Arthritis Rheum 2001;44:1545–54.
7. Gao W, Sweeney C, Connolly M, Kennedy A, Ng CT, McCormick J, et al. Notch-1 mediates hypoxia-induced angiogenesis in rheumatoid arthritis. Arthritis Rheum 2012;64:2104–13.
8. Gao W, Sweeney C, Walsh C, Rooney P, McCormick J, Veale D, et al. Notch signalling pathways mediate synovial angiogenesis in response to vascular endothelial growth factor and angiopoietin 2. Ann Rheum Dis 2013;72:1080–8.
9. Jiao Z, Wang W, Ma J, Wang S, Su Z, Xu H. Notch signaling mediates TNF-α-induced IL-6 production in cultured fibroblast-like synoviocytes from rheumatoid arthritis. Clin Dev Immunol 2012;2012:350209.
10. Wongchana W, Palaga T. Direct regulation of interleukin-6 expression by Notch signaling in macrophages. Cell Mol Immunol 2011;9:155–62.
11. Gentle M, Rose A, Bugeon L, Dallman M. Noncanonical Notch signaling modulates cytokine responses of dendritic cells to inflammatory stimuli. J Immunol 2012;189:1274–84.
12. Okamoto M, Matsuda H, Joetham A, Lucas J, Domenico J, Yasutomo K, et al. Jagged1 on dendritic cells and Notch on $CD4^+$ T cells initiate lung allergic responsiveness by inducing IL-4 production. J Immunol 2009;183:2995–3003.
13. Hardy R, Hulso C, Liu Y, Gasparini S, Fong-Yee C, Tu J, et al. Characterisation of fibroblast-like synoviocytes from a murine model of joint inflammation. Arthritis Res Ther 2013;15:R24.
14. Sekine C, Sugihara T, Miyake S, Hirai H, Yoshida M, Miyasaka N, et al. Successful treatment of animal models of rheumatoid arthritis with small-molecule cyclin-dependent kinase inhibitors. J Immunol 2008;180:1954–61.
15. Moriyama Y, Sekine C, Koyanagi A, Koyama N, Ogata H, Chiba S, et al. Delta-like 1 is essential for the maintenance of marginal zone B cells in normal mice but not in autoimmune mice. Int Immunol 2008;20:763–73.
16. Sekine C, Moriyama Y, Koyanagi A, Koyama N, Ogata H, Okumura K, et al. Differential regulation of splenic CD8- dendritic cells and marginal zone B cells by Notch ligands. Int Immunol 2009;21:295–301.
17. Kamata K, Kamijo S, Nakajima A, Koyanagi A, Kurosawa H, Yagita H, et al. Involvement of TNF-like weak inducer of apoptosis in the pathogenesis of collagen-induced arthritis. J Immunol 2006;177:6433–9.
18. Korganow AS, Ji H, Mangialaio S, Duchatelle V, Pelanda R, Martin T, et al. From systemic T cell self-reactivity to organ-specific autoimmune disease via immunoglobulins. Immunity 1999;10:451–61.
19. Maccioni M, Zeder-Lutz G, Huang H, Ebel C, Gerber P, Hergueux J, et al. Arthritogenic monoclonal antibodies from K/BxN mice. J Exp Med 2002;195:1071–7.
20. Ji H, Rettit A, Ohmura K, Ortiz-Lopez A, Duchatelle V, Degott C, et al. Critical roles for interleukin 1 and tumor necrosis factor α in antibody-induced arthritis. J Exp Med 2002;196:77–85.
21. Burmester GR, Weinblatt ME, McInnes IB, Porter D, Barbarash O, Vatutin M, et al, for the EARTH Study Group. Efficacy and safety of mavrilimumab in subjects with rheumatoid arthritis. Ann Rheum Dis 2013;72:1445–52.
22. Cook AD, Turner AL, Braine EL, Pobjoy J, Lenzo JC, Hamilton JA. Regulation of systemic and local myeloid cell subpopulations by bone marrow cell–derived granulocyte–macrophage colony-stimulating factor in experimental inflammatory arthritis. Arthritis Rheum 2011;63:2340–51.
23. Hicks C, Johnston SH, diSibio G, Collazo A, Vogt TF, Weinmaster G. Fringe differentially modulates Jagged1 and Delta1 signalling through Notch1 and Notch2. Nat Cell Biol 2000;2:515–20.
24. Stanley P. Regulation of Notch signaling by glycosylation. Curr Opin Struct Biol 2007;17:530–5.
25. Tan JB, Xu K, Cretegny K, Visan I, Yuan JS, Egan SE, et al. Lunatic and Manic Fringe cooperatively enhance marginal zone B cell precursor competition for Delta-like 1 in splenic endothelial niches. Immunity 2009;30:254–63.

arthritis research&therapy

RESEARCH ARTICLE Open Access

Abrogation of CC chemokine receptor 9 ameliorates collagen-induced arthritis of mice

Waka Yokoyama[1], Hitoshi Kohsaka[1], Kayoko Kaneko[1], Matthew Walters[2], Aiko Takayasu[1], Shin Fukuda[1], Chie Miyabe[1,3], Yoshishige Miyabe[1], Paul E Love[4], Nobuhiro Nakamoto[5], Takanori Kanai[5], Kaori Watanabe-Imai[1], Trevor T Charvat[2], Mark ET Penfold[2], Juan Jaen[2], Thomas J Schall[2], Masayoshi Harigai[1], Nobuyuki Miyasaka[1] and Toshihiro Nanki[1,6*]

Abstract

Introduction: Biological drugs are effective in patients with rheumatoid arthritis (RA), but increase severe infections. The CC chemokine receptor (CCR) 9 antagonist was effective for Crohn's disease without critical adverse effects including infections in clinical trials. The present study was carried out to explore the pathogenic roles of chemokine (C-C motif) ligand (CCL) 25 and its receptor, CCR9, in autoimmune arthritis and to study if the CCR9 antagonist could be a new treatment for RA.

Methods: CCL25 and CCR9 expression was examined with immunohistochemistry and Western blotting. Concentration of interleukin (IL)-6, matrix metalloproteinase (MMP)-3 and tumor necrosis factor (TNF)-α was measured with enzyme-linked immunosorbent assays. Effects of abrogating CCR9 on collagen-induced arthritis (CIA) was evaluated using CCR9-deficient mice or the CCR9 antagonist, CCX8037. Fluorescence labeled-$CD11b^+$ splenocytes from CIA mice were transferred to recipient CIA mice and those infiltrating into the synovial tissues of the recipient mice were counted.

Results: CCL25 and CCR9 proteins were found in the RA synovial tissues. CCR9 was expressed on macrophages, fibroblast-like synoviocytes (FLS) and dendritic cells in the synovial tissues. Stimulation with CCL25 increased IL-6 and MMP-3 production from RA FLS, and IL-6 and TNF-α production from peripheral blood monocytes. CIA was suppressed in CCR9-deficient mice. CCX8037 also inhibited CIA and the migration of transferred $CD11b^+$ splenocytes into the synovial tissues.

Conclusions: The interaction between CCL25 and CCR9 may play important roles in cell infiltration into the RA synovial tissues and inflammatory mediator production. Blocking CCL25 or CCR9 may represent a novel safe therapy for RA.

Introduction

Rheumatoid arthritis (RA) is characterized by persistent and erosive arthritis in multiple joints. The accumulation of a large number of T cells and macrophages [1-3], proliferation of fibroblast-like synoviocytes (FLS), production of inflammatory mediators and activation of osteoclasts are revealed in the affected joints and lead to destruction of the joints with pain and daily disability [4-8]. Biological drugs, such as tumor necrosis factor (TNF) blockers and interleukin (IL)-6 receptor antagonists, are effective in patients with RA [9-11]. Since the risk of severe infections is increased by biological drugs [12-14], safer therapies for RA should be developed.

As a new treatment, anti-chemokine therapy has been intensively studied for inflammatory diseases. Chemokines are a family of small secreted molecules that induce directed chemotaxis of responding cells and activation of inflammatory cells [15-17]. According to the results of a large phase II study, the CC chemokine receptor (CCR) 9 antagonist, CCX282-B was effective for Crohn's disease

* Correspondence: nanki@med.teikyo-u.ac.jp
[1]Department of Rheumatology, Graduate School of Medical and Dental Sciences, Tokyo Medical and Dental University, 1-5-45, Yusima, Bunkyo-ku, Tokyo 110-8519, Japan
[6]Department of Clinical Research Medicine, Teikyo University, 2-11-1 Kaga, Itabashi-ku, Tokyo 173-8605, Japan
Full list of author information is available at the end of the article

without critical adverse effects [18,19]. Especially, this treatment did not increase the risk of infections for 12 months. CCR9, a unique receptor for chemokine (C-C motif) ligand (CCL) 25, is expressed on lymphocytes of intestinal lamina propria and intraepithelial and dendritic cells (DCs) in the small intestine and thymocytes [20,21]. CCL25 is expressed by the follicle-associated epithelium of Peyer's patches, the crypts of Lieberkühn in the small intestine and the thymus [21,22]. Physiologically, the interaction between CCL25 and CCR9 contribute to the T cell and DC migration into the small intestine and movement of T cells in the thymus.

It was reported that CCR9 expression on cell surface of peripheral blood monocytes from RA patients was higher than that from healthy donors [23]. CCR9 and CCL25 were expressed on macrophages in the RA synovial tissues [23]. These data suggest that interaction of CCL25 and CCR9 may contribute to the inflammatory cell migration into the RA synovial tissues. Although blockade of CCL25 and CCR9 interaction might also be applicable to RA, the pathogenic roles of these molecules in RA have been little known.

In this study, we examined the stimulatory effects of CCL25 on FLS and monocytes and effects of the abrogation of CCR9 on a murine model of RA.

Methods

Specimens

Synovial tissue samples were obtained from eleven RA patients who fulfilled the American College of Rheumatology classification criteria for RA [24] and seven patients with osteoarthritis (OA) who underwent total knee joint replacement. Nine RA patients were positive for rheumatoid factor (81%) and ten were positive for anti-citrullinated protein antibodies (91%). All subjects provided written informed consent. The experimental protocols were approved by the Ethics Committee of Tokyo Medical and Dental University.

Immunodetection

Mouse anti-CCR9 (248621: R&D Systems, Minneapolis, MN, USA), CCL25 (52513: R&D Systems), or β-actin (AC-15: Sigma-Aldrich, St Louis, MO, USA) monoclonal antibody (mAb) was used as a primary antibody for Western blotting [25]. Immunohistochemistry was conducted as described previously [25]. Frozen sections fixed with ice-cold acetone was blocked with Tris-buffered saline, 2% goat serum, 1% bovine serum albumin, 0.1% Triton X-100, and 0.05% Tween-20. Mouse anti-CCR9, CCL25 mAb (10 μg/ml: R&D Systems) or isotype control was used as a primary antibody. Alexa Fluor™ 546-conjugated goat anti-mouse IgG2a or IgG2b Ab (4 μg/ml: Invitrogen, Carlsbad, CA, USA) was used as a secondary antibody. For double immunohistochemistry, the sections were also stained with mouse anti-CD68 (10 μg/ml: KP1; Dako, Glostrup, Denmark), cadherin-11 (1 μg/ml: 16A; Acris Antibodies, Hiddenhausen, Germany), or dendritic cell lysosome-associated membrane glycoprotein (DC-LAMP) (10 μg/ml: 104.G4; Immunotec Inc., Quebec, Canada) mAb. They were then incubated with 4 μg/ml Alexa Fluor™ 488-conjugated goat anti-mouse IgG1 (Invitrogen). A nuclear stain was performed with 4', 6-diamidino-2-phenylindole. To determine the percentages of CCR9-expressed cells, the number of CCR9-positive cells in CD68-, cadherin-11-, or DC-LAMP-positive cells was counted in three randomly selected fields examined at x200 magnification under fluorescence microscope.

Cell culture

FLS was established from the RA and OA synovial tissues and used for experiments after five passages [26]. The cells did not express CD14 or human leukocyte antigen class II, suggesting that macrophages and DCs were not contained in the FLS [26]. Human peripheral blood $CD14^+$ monocytes from healthy donors were purified by magnetic-activated cell sorting microbeads coupled with mAb and magnetic cell separation columns (Miltenyi Biotec, Bergisch Gladbach, Germany). The purity of $CD14^+$ monocytes was more than 95%. CCR9 expression of RA FLS and purified human peripheral blood monocytes was evaluated with phycoerythrin-conjugated anti-CCR9 mAb (112509: R&D Systems) or the isotype control staining using an Accuri C6 flow cytometer (Accuri Cytometers, BD Biosciences, San Jose, CA, USA). RA FLS were cultured with 10% fetal calf serum (FCS) for 48 hours with or without recombinant human CCL25 (R&D Systems). Purified human peripheral blood monocytes were cultured with 10% FCS for 24 hours with or without CCL25. Concentrations of IL-6, matrix metalloproteinase (MMP)-3 and TNF-α in the culture supernatants were measured with enzyme-linked immunosorbent assay (ELISA) kits (DuoSet: R&D Systems).

Induction and treatment of collagen-induced arthritis (CIA)

To induce CIA, 10-week-old CCR9-deficient mice [27] and wild-type (WT) mice with a C57BL/6 J background were treated with chicken type II collagen (CII; Sigma-Aldrich) [28]. Eight-week-old DBA/1 J mice were treated with bovine CII (Collagen Research Center, Kiel, Germany) [29]. Disease severity was evaluated with the clinical arthritis score, incidence of arthritis, pathological score [29] and radiological score. Bone destruction was evaluated with bone erosion of the bilateral foot joints as follows: 0 = not obvious erosion, 1 = one erosion, 2 = two erosions, 3 = more than three erosions, and if a bone deformity was seen in the foot joint, one point was added (to a maximum of eight points).

DBA/1 J mice with CIA were injected subcutaneously with selective CCR9 antagonist, CCX8037 [30] or vehicle alone. Migration of $CD11b^+$ splenocytes into synovial tissues of CIA mice was evaluated as described previously [31,32]. CD11b-positive splenocytes from CIA mice were purified using magnetic-activated cell sorting microbeads coupled with mAb and magnetic cell separation columns (Miltenyi Biotec). The purified CD11b cells were labeled with CellTracker™ Orange 5-(and-6)-(((4-chloromethyl) benzoyl) amino) tetramethylrhodamine (CMTMR: Molecular Probes, Eugene, OR, USA) according to the protocol supplied by the manufacturer. The CMTMR-labeled 1×10^7 cells were intravenously injected into the tail vein of CIA mice at day 9. The recipient mice were treated with CCX8037 (10 mg/kg in 1% hydroxyprophyl methylcellulose) or vehicle 24 hours, 12 hours, and 30 minutes before the transfer, and 12 hours after the transfer. After 24 hours, ankle joints were harvested, embedded in glycol methacrylate, and sagittal 3-μm-thick microtome sections were prepared. The numbers of CMTMR-labeled cells that migrated into the synovium between tibiotalar and tarsometatarsal joints were counted under fluorescent microscopy. The experiment protocols were approved by the Institutional Animal Care and Use Committee of Tokyo Medical and Dental University.

Statistical analysis

To compare three or more groups, including results of concentration of inflammatory mediators, area under the curve (AUC) by arthritis score, histological and radiological scores by therapeutical treatment, a one-way analysis of variance (ANOVA) test was used. To compare arthritis score, a two-way ANOVA test was used. AUC by arthritis score, histological score and radiographic score by prophylactic treatment or experiments using CCR9-deficient mice, and number of migrated $CD11b^+$ splenocytes, Student's *t* test was also applied. A *P* value less than 0.05 was considered statistically significant.

Results

Expression of CCR9 and CCL25 in the RA synovial tissues

CCR9 expression in RA and OA synovial tissues was evaluated with Western blotting. The CCR9 protein was found more in the RA synovial tissues than in the OA synovial tissues (Figure 1A). Immunohistochemical analyses of the RA synovial tissues revealed that most $CD68^+$ macrophages expressed CCR9 (Figure 1B-D), which is consistent with previous reports [23]. To examine the proportion of CCR9-expressed cells, the number of CCR9-positive cells in 218.83 ± 24.11 $CD68^+$ cells (n =3), 206.33 ± 23.08 cadherin-11^+ cells (n =3) and 11.33 ± 0.53 DC-$LAMP^+$ cells (n =3) was counted. The percentage of CCR9-positive cells in $CD68^+$ macrophages was $76.1 \pm 5.3\%$. In addition, cadherin-11^+ FLS and DC-$LAMP^+$ DCs also expressed CCR9 ($67.1 \pm 8.3\%$, $11.4 \pm 15.2\%$, respectively) (Figure 1E- J).

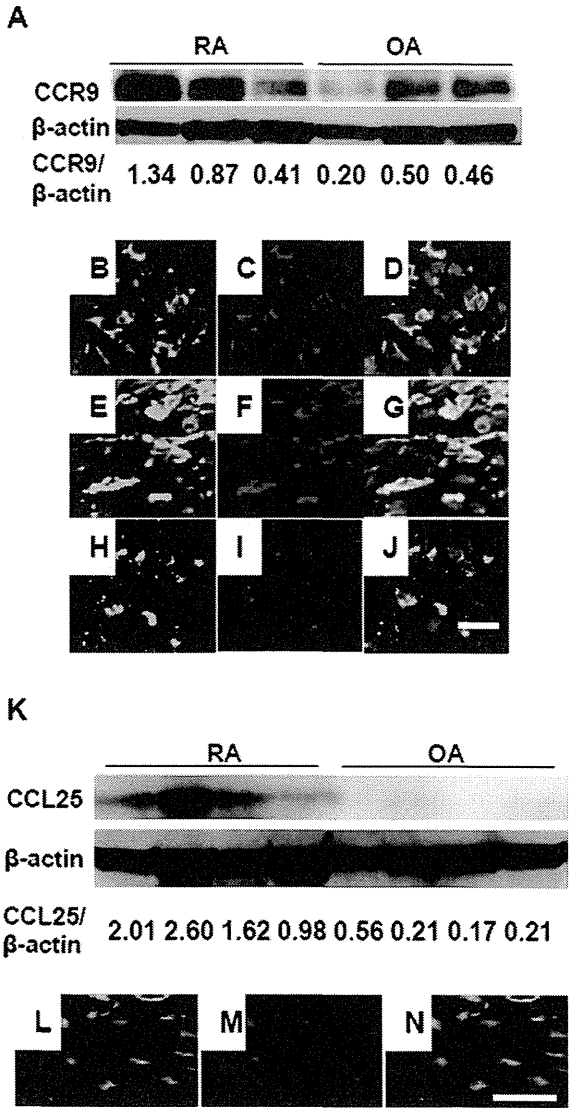

Figure 1 CCR9 and CCL25 expression in the RA synovial tissues. **(A)** Western blots of CCR9 protein expression in three RA and three OA synovial tissues. Ratio of CCR9/β-actin protein level is indicated below. **(B-J)** Sections of RA synovial tissue were double-stained with CCR9 and CD68, cadherin-11 and DC-LAMP (B, CD68; C, CCR9; D, merged B with C; E, cadherin-11; F, CCR9; G, merged E with F; H, DC-LAMP; I, CCR9; J, merged H with I). Bar, 20 μm. **(K)** Western blots of CCL25 protein expression in four RA and four OA synovial tissues. Ratio of CCL25/β-actin protein level is indicated below. **(L-N)** Sections of RA synovial tissue were double-stained with CCL25 and CD68 (L, CD68; M, CCL25; N, merged L with M). Bars, 20 μm. CCL, chemokine (C-C motif) ligand; CCR, CC chemokine receptor; DC-LAMP, dendritic cell lysosome-associated membrane glycoprotein; OA, osteoarthritis; RA, rheumatoid arthritis.

The CCL25 expression in RA and OA synovial tissues was analyzed with Western blotting. CCL25 was expressed more in the RA synovial tissues than in the OA synovial

tissues (Figure 1K). Double immunohistochemistry revealed that $CD68^+$ macrophages expressed CCL25 in the RA synovial tissues (Figure 1L-N), which is consistent with previous reports [23].

Stimulatory effects of CCL25 on RA FLS and human peripheral blood monocytes

Since FLS expressed CCR9 in the RA synovial tissues, we examined the stimulatory effects of CCL25 on the cultured RA FLS, which also expressed CCR9 (Figure 2A; mean fluorescence intensity (MFI) for CCR9: 157,963 ± 37,811, MFI for isotype control: 70,914 ± 3,163 (mean ± standard error of the mean (SEM)), n =3). We cultured RA FLS for 48 hours with various concentrations of CCL25. Stimulation with CCL25 increased IL-6 and MMP-3 levels in the culture supernatants in a dose-dependent manner (Figure 2B). Production of TNF-α was not detected by unstimulated or CCL25-stimulated RA FLS. We next examined the effect of CCL25 on IL-6 and MMP-3 production by OA FLS. IL-6 and MMP-3 were also secreted from unstimulated OA FLS, although the levels were lower than those from RA FLS (IL-6; RA: 1,393 ± 493 mg/dl (n =3), OA: 171 ± 83 mg/dl (n =2), P <0.05, MMP-3; RA: 2135 ± 644 mg/dl, OA: 296 ± 50 mg/dl, P <0.05). IL-6 secretion from OA FLS was slightly increased by CCL25, although it was not statistically significant (CCL25 5 ng/ml: 185 ± 93 mg/dl, 50 ng/ml: 206 ± 120 mg/dl, 500 ng/ml: 243 ± 123 mg/dl). Production of MMP-3 from OA FLS was not significantly altered by CCL25 (CCL25 5 ng/ml: 324 ± 115 mg/dl, 50 ng/ml: 324 ± 65 mg/dl, 500 ng/ml: 312 ± 112 mg/dl).

Instead of the synovial macrophages, which were not available on a large scale, we examined the effect of CCL25 on human peripheral blood monocytes. They also expressed CCR9 (Figure 3A; MFI for CCR9: 24,149 ± 13,536, MFI for isotype control: 2,038 ± 1,265, n =3) and were cultured for 24 hours with various concentrations of CCL25. This treatment promoted IL-6 and TNF-α production in a dose-dependent manner (Figure 3B).

Effects of CCR9 gene deletion on murine CIA

The above data prompted us to investigate the effect of the abrogation of CCR9 on murine CIA. We analyzed the development of CIA in CCR9-deficient mice. The clinical arthritis scores in the CCR9-deficient mice were significantly lower than those in the WT (Figure 4A). AUC by the arthritis score was calculated. The AUC tended to be smaller in CCR9-deficient mice compared to WT mice, although the difference was not statistical significant (WT: 13.40 ± 17.75, CCR9-deficient: 4.08 ± 10.34). Histological and radiographic examinations revealed that mononuclear cell infiltration and bone destruction were inhibited in the CCR9-deficient mice (Figure 4B and C).

Effects of the CCR9 antagonist on murine CIA

Next, we investigated the effect of the CCR9 antagonist, CCX8037, on murine CIA. To analyze its effects in a preventive protocol, CCX8037 (3 mg/kg or 10 mg/kg) or vehicle alone was injected subcutaneously twice daily from 7 days prior to the second immunization to 14 days after the immunization. This treatment significantly inhibited clinical arthritis score in a dose-dependent manner (Figure 5A). AUC by the arthritis score was also significantly smaller by CCX8037 (10 mg/kg)-treated mice compared with vehicle-treated mice (vehicle: 17.67 ± 11.78, CCX8037 3 mg/kg: 13.67 ± 11.79 (not significant, vs. vehicle), CCX8037 10 mg/kg: 6.79 ± 9.22 (P =0.01, vs. vehicle)). Moreover, CCX8037 significantly inhibited mononuclear cell infiltration and bone destruction (Figure 5B and C).

To investigate the effects of CCX8037 in a therapeutic protocol, we injected CIA mice with CCX8037 10 mg/kg or vehicle alone 5 days after the second immunization for 13 days. CCX8037 significantly inhibited arthritis, mononuclear cell infiltration and bone destruction (Figure 5D-F). AUC by the arthritis score was also significantly smaller in CCX8037-treated mice compared with vehicle-treated mice (vehicle: 30.50 ± 16.46, CCX8037 10 mg/kg: 14.46 ± 10.75 (P <0.01, vs. vehicle)).

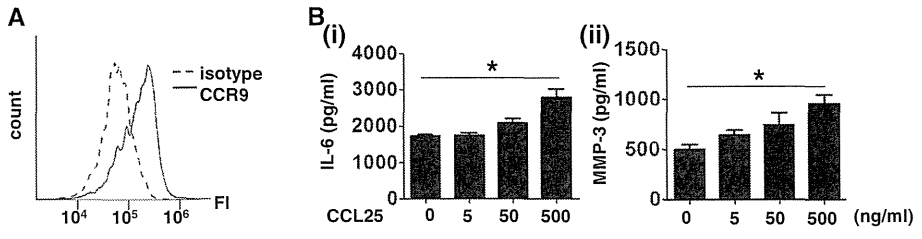

Figure 2 Effects of CCL25 on cultured RA FLS. (A) CCR9 expression on *in vitro* cultured RA FLS was determined by flow cytometry. Horizontal line indicates fluorescence intensity (FI). **(B)** RA FLS were cultured for 48 hours with various concentrations of CCL25. Concentrations of IL-6 (i) and MMP-3 (ii) in the culture supernatant were measured with ELISA. Values are the mean ± SEM of three independent experiments. *P <0.05. CCL, chemokine (C-C motif) ligand; CCR, CC chemokine receptor; ELISA, enzyme-linked immunosorbent assay; FLS, fibroblast-like synoviocytes; IL, interleukin; MMP, metalloproteinase; RA, rheumatoid arthritis; SEM, standard error of the mean.

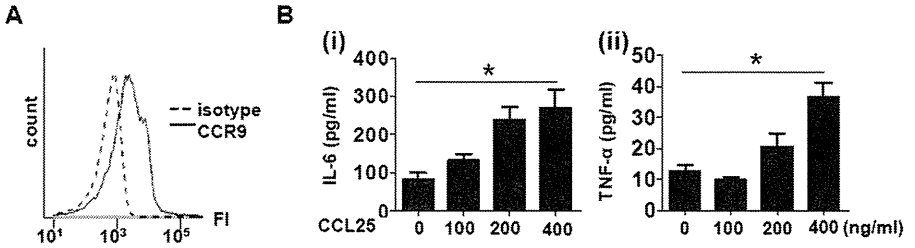

Figure 3 Effects of CCL25 on human peripheral blood monocytes. (A) CCR9 expression on peripheral blood $CD14^+$ monocytes was analyzed with flow cytometry. **(B)** Monocytes were cultured for 24 hours with various concentrations of CCL25. Concentrations of IL-6 (i) and TNF-α (ii) in the culture supernatant were measured with ELISA. Values are the mean ± SEM of three independent experiments. *P <0.05. CCL, chemokine (C-C motif) ligand; CCR, CC chemokine receptor; ELISA, enzyme-linked immunosorbent assay; IL, interleukin; SEM, standard error of the mean; TNF, tumor necrosis factor.

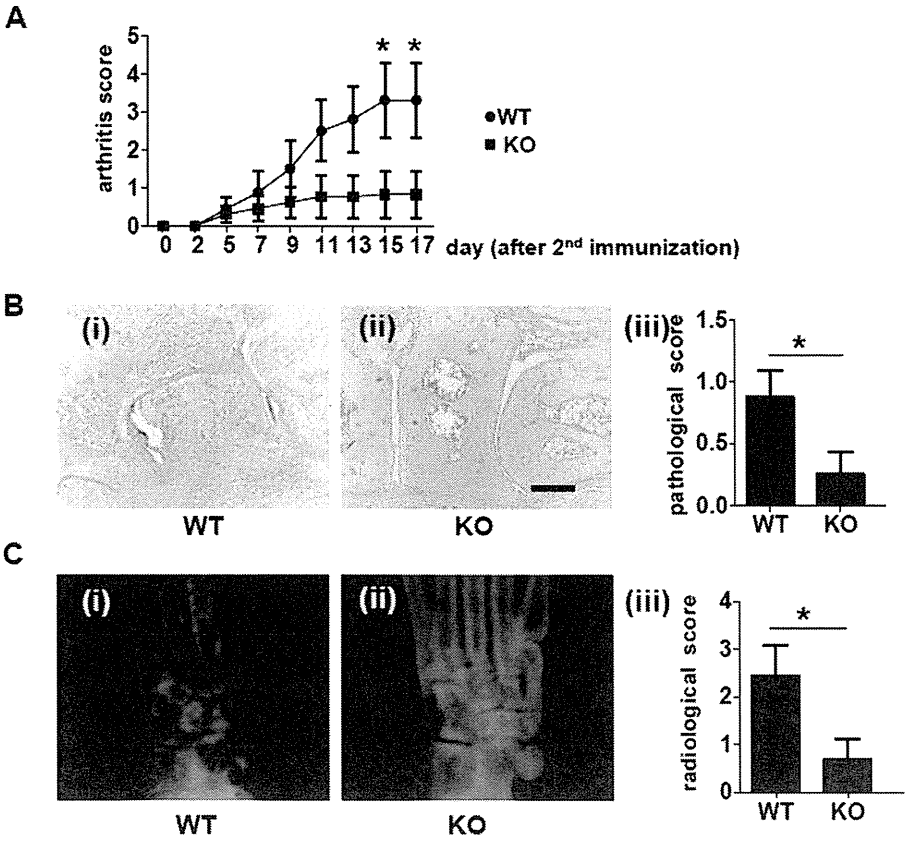

Figure 4 Suppressed CIA in CCR9-deficient mice. (A-C) CCR9-deficient mice (knockout (KO)) (n =13) and WT mice (n =16) were immunized with chicken CII on day −21 and 0. Day 0 means the day of the second immunization. Disease severity was recorded as the clinical arthritis score until day 18 (A). Ankle joints on day 18 from KO (B(i)) and WT mice (B(ii)) were stained with hematoxylin and eosin. Bar, 300 μm. Inflammatory cell infiltration in the right ankle joint was scored with a pathological score (B(iii)). Representative radiographs of the ankle joints of KO (C(i)) and WT mice (C(ii)). Bone erosion in the bilateral ankle joints was scored with radiological score (C(iii)). Representative photomicrographs are shown. Values are the mean ± SEM of each group. *P <0.05 versus WT. CCR, CC chemokine receptor; CIA, collagen-induced arthritis; CII, type II collagen; SEM, standard error of the mean; WT, wild-type.

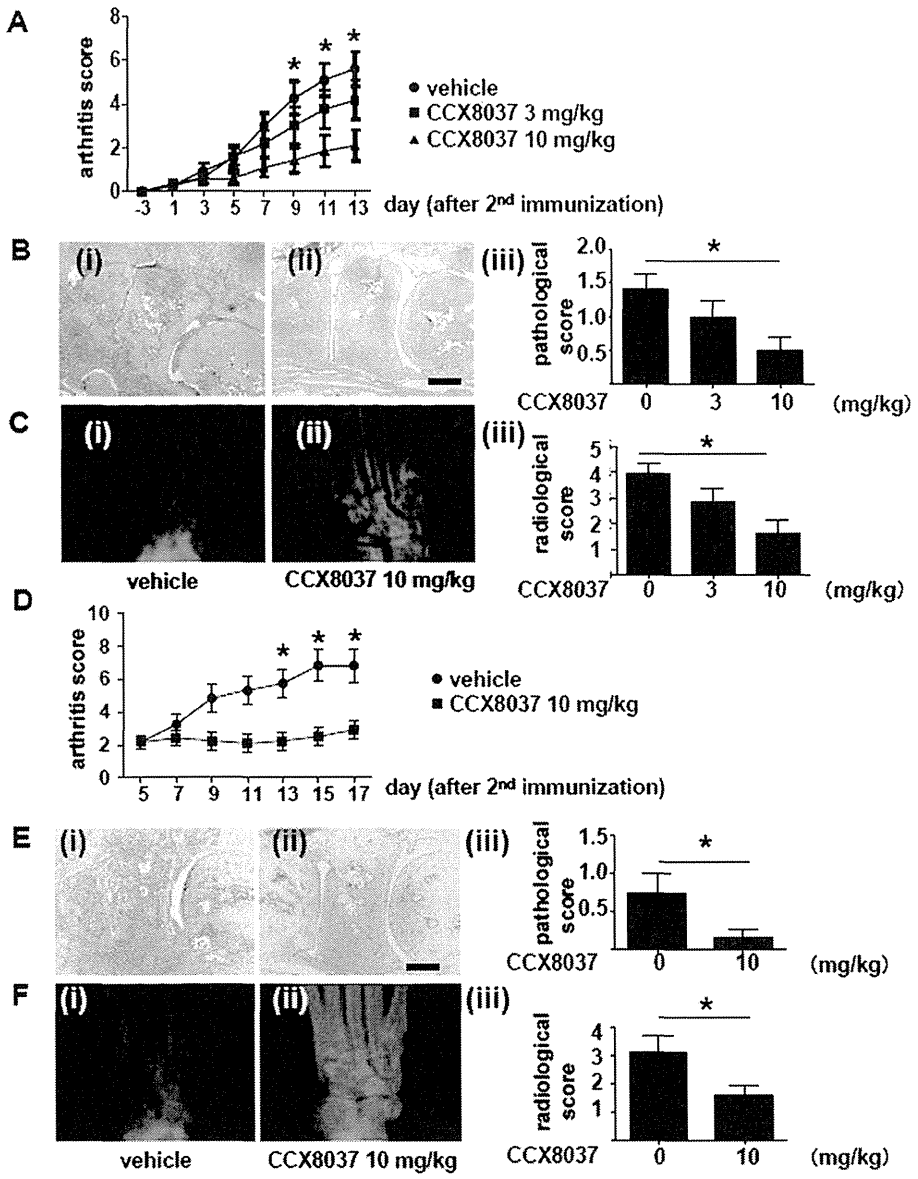

Figure 5 Effects of CCX8037 on CIA mice. (A-C) CCX8037 (3 mg/kg or 10 mg/kg) or vehicle (all n =12) was injected subcutaneously twice daily from day −7 to day 14. Disease severity was recorded as the clinical arthritis score until day 14 (A). Representative photographs showing hematoxylin and eosin staining of the ankle joints from mice with CIA treated with vehicle (B(i)) or CCX8037 (10 mg/kg) (B(ii)). Bar, 300 μm. Inflammatory cell infiltration in the right ankle joint was scored with a pathological score (B(iii)). Representative radiographs of the ankle joints of CIA mice treated with vehicle (C(i)) or CCX8037 (10 mg/kg) (C(ii)). Bone erosion in the bilateral ankle joints was scored with radiological score (C(iii)). Values are the mean ± SEM of each group. *P <0.05, CCX8037 (10 mg kg) versus vehicle. **(D-F)** To investigate the therapeutic effects of CCX8037, at day 5 after the second immunization, mice were divided into two groups with equal average arthritis score. CCX8037 (10 mg/kg) or vehicle (all n =12) was injected subcutaneously twice daily from day 5 to day 18. Disease severity was recorded as the clinical arthritis score (D). Representative hematoxylin and eosin staining of the ankle joints of CIA mice treated with vehicle (E(i)) or CCX8037 (10 mg/kg) (E(ii)). Bar, 300 μm. Pathological score (E(iii)). Representative radiographs of the ankle joints of CIA mice treated with vehicle (F(i)) or CCX8037 (10 mg/kg) (F(ii)). Radiological score (F(iii)). Values are the mean ± SEM of each group. *P <0.05 versus vehicle. CCX8037, CC chemokine receptor (CCR) 9 antagonist; CIA, collagen-induced arthritis; SEM, standard error of the mean.

The CCR9 antagonist inhibited migration of CD11b$^+$ splenocytes

In the RA synovial tissues, most macrophages expressed CCR9, and CCL25 was abundant (Figure 1B-D and 1K). It was reported that CCL25 induced migration of monocytes/macrophages *in vitro* [23,33,34], indicating that the interaction of CCL25 and CCR9 may have an important role in the migration of monocytes into the inflamed synovial tissues.

We then analyzed the effect of CCR9 blockade on inflammatory cell migration *in vivo*. We showed previously that CD11b$^+$ macrophages from CIA mice labeled and

transferred to the recipient CIA mice were identified in the inflamed synovial tissues of the recipients [31,32]. $CD11b^+$ splenocytes express CCR9 [35]. To analyze the effect of CCX8037 on the macrophages migration, recipient mice were treated with CCX8037 or vehicle 24 hours, 12 hours, and 30 minutes before the cell transfer, and 12 hours after the transfer. Twenty-four hours after the transfer, the number of labeled cells in the synovial tissues was counted. Although, this short-term treatment did not alter the arthritis severity of the recipient mice, the treated mice had significantly reduced number of the migrated cells in the synovial tissues in contrast to the vehicle-treated group (Figure 6).

Discussion

In this study, we showed that the abrogation of CCR9 ameliorated arthritis in a murine model of RA. We also found that the *in vivo* migration of macrophages was suppressed by the administration of CCX8037. In addition, we showed stimulatory effects of CCL25 on the production of inflammatory mediators from RA FLS and human peripheral blood monocytes *in vitro*. The results suggest that CCR9 could be a therapeutic target for RA.

As was reviewed earlier, chemokines are apparent therapeutic targets in RA treatment. Especially, CCR1, CCR2 and CCR5 are abundantly expressed on RA synovial macrophages and the validity of CCR1, CCR2 and CCR5 antagonist for the animal model of arthritis has been studied. CCR1 antagonist was effective in a clinical trial [36], while blockade of CCL2, CCR2 or CCR5 was not [37-39]. In the trial of CCR2 or CCR5 antagonist, no significant reduction in numbers of macrophages in the synovial tissues was observed, suggesting that CCR2 and CCR5 may not play a critical role in the migration of monocytes. In addition, since CCR2 and CCR5 are expressed on regulatory T cells, their blockade might inhibit regulatory T cells that suppressed the disease.

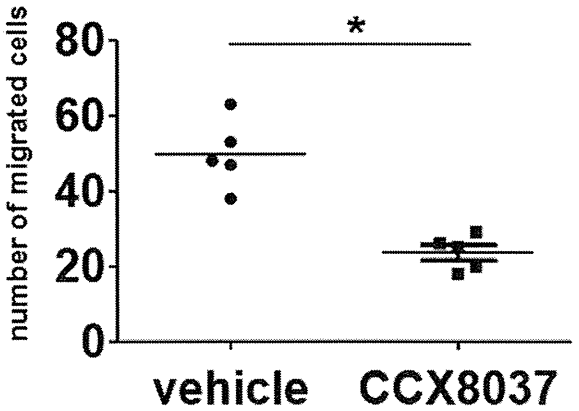

Figure 6 Effect of CCX8037 on the migration of $CD11b^+$ splenocytes into the joints. Cell Tracker Orange CMTMR-labeled $CD11b^+$ splenocytes from CIA mice (1×10^7) were adoptively transferred into each recipient CIA mouse on day 9 after the second immunization. The recipient mice were treated with CCX8037 (10 mg/kg in 1% hydroxyprophyl methylcellulose) or vehicle 24 hours, 12 hours, and 30 minutes before the transfer, and 12 hours after the transfer. Twenty-four hours after the transfer, ankle joints were harvested and examined for migrated cells under a fluorescent microscope. The total number of labeled cells in three fields of vision was counted in the synovial tissue between the tibiotalar and transmetatarsal joints (n =5) at x20 magnification. Horizontal bars indicate the mean of each group. *P <0.001 versus vehicle. CCX8037, CC chemokine receptor (CCR) 9 antagonist; CIA, collagen-induced arthritis; CMTMR; 5-(and-6)-(((4-chloromethyl) benzoyl) amino) tetramethylrhodamine.

CCR9 was expressed on FLS, macrophages and DCs in the RA synovial tissues. This should be driven by inflammatory cytokines in the synovial tissues, since stimulation with TNF-α increased CCR9 expression on THP monocytic cells [23]. CCR9 was also expressed on *in vitro* cultured RA FLS and peripheral blood monocytes from healthy donors. CCL25 stimulated them to produce inflammatory mediators that are important in the pathogenesis of RA. CCL25 should exacerbate arthritis via these effects in addition to the inflammatory cell recruitment. We could not measure CCL25 concentration in the RA synovial tissue. However, chemokines bind surface proteoglycans [40], and they could be sequestered and presented to target cells at high concentration in the local microenvironment.

In vivo macrophage migration was suppressed by CCR9 inhibition, which might have a great impact on inhibition of CIA. It was shown that $CD3^+$ T cells and $CD20^+$ B cells in the RA synovial tissues did not express CCR9 [23]. In addition, the serum concentration of anti-CII IgG1, IgG2a and IgG2b in the CCX8037-treated group was not lower than the vehicle group both in the preventive and therapeutic treatment experiments (data not shown). The effect of CCX8037 may not depend on the inhibition of T and B cells recruitment into the synovial tissues or reduction of antibody production. It was reported that deficiency of CCR9, as well as CCR1, CCR2 and CCR5, did not attenuate a murine model of serum transfer arthritis [41]. It is believed that innate immune system is important for serum transfer arthritis, while adaptive immune system is important for CIA. Macrophages and neutrophils are essential for serum transfer arthritis [41,42]. Reduction in the number of macrophages in the synovial tissues might not have enough of an impact to suppress the inflammation of arthritis in serum transfer arthritis, while that might suppress CIA. On the other hand, CCR9 was expressed on the $DC\text{-}LAMP^+$ cell in the synovial tissues, which is a mature DC [43] in the RA synovial tissues. We did not investigate the effect of the CCL25-CCR9 interaction on DCs in this study. Further studies are needed to investigate the regulation of CCR9 expression and effect of CCL25 stimulation on DCs.